ORIENTATION OF MOLECULAR SOLUTES

IN NEMATIC LIQUID CRYSTALS:

SIZE AND SHAPE EFFECTS

by

KOK, MEI YENG

B.Sc. (Hons.), The University of British Columbia, 1985

A THESIS SUBMITTED IN PARTIAL FULFILLMENT OF

THE REQUIREMENTS FOR THE DEGREE OF

MASTER OF SCIENCE

in

THE FACULTY OF GRADUATE STUDIES

(Department of Chemistry)

We accept this thesis as conforming

to the required standard

THE UNIVERSITY OF BRITISH COLUMBIA
SEPTEMBER, 1986

© Kok, Mei Yeng, 1986

In presenting this thesis in partial fulfilment of the
requirements for an advanced degree at the University
of British Columbia, I agree that the Library shall make
it freely available for reference and study. I further
agree that permission for extensive copying of this thesis
for scholarly purposes may be granted by the head of my
department or by his or her representatives. It is
understood that copying or publication of this thesis
for financial gain shall not be allowed without my written
permission.

Department of _____CHEMISTRY_____

The University of British Columbia
1956 Main Mall
Vancouver, Canada
V6T 1Y3

Date _____Oct 17th, 1986_____

ABSTRACT

An understanding of the mechanisms of orientation of solutes in anisotropic solvents is of fundamental importance in the theory of liquid crystalline systems. A systematic study of these mechanisms is presently being conducted in this and other laboratories. As part of this investigation, the orientational order of a series of C_{2v} solutes in the liquid crystal mixture 55 wt% 1132 (Merck ZLI 1132) and 45 wt% partially deuterated EBBA (N-(4-ethoxybenzylidene)-2,6-dideutero-4-n-butylaniline) was studied using NMR spectroscopy. This technique provides a description of the average orientation of a solute in terms of the order parameters. The results obtained indicate a good correlation between order parameters and the size and shape of the solutes. A model based on short range hard body interactions, which depend on the dimensions of the solute, was used to predict orientational ordering. Excellent agreement was obtained between observed and calculated order parameters. These results provide supportive evidence that the mechanism responsible for orientation in the 55 wt% 1132 system is short range hard body interactions.

A side study was conducted on the ordering of furan and thiophene in the liquid crystalline solvents 1132 and EBBA. Temperature dependence of order parameters in 55 wt% 1132 were examined. Orientation in 1132 and EBBA and temperature dependence in 55 wt% 1132 can be explained in terms of:

(i) the short range interactions dependent on the dimensions of the

solute, and

(ii)   the   interaction between   the   molecular quadrupole moment of the
solute and the average electric field gradient which is due to the
solvent.

TABLE OF CONTENTS

LIST OF TABLES

LIST OF FIGURES

LIST OF ABBREVIATIONS

EBBA	-	N-(4-ethoxybenzylidene)-4-n-butylaniline
1132	-	Merck ZLI 1132 : mixture of $C_{16}H_{21}N$, $C_{18}H_{25}N$, $C_{20}H_{29}N$, $C_{24}H_{29}N$.
55 wt% 1132	-	Mixture of 1132-EBBA, weight composition: 55% 1132 and 45% EBBA.
NMR	-	Nuclear magnetic resonance
TTF	-	Tetrathiofulvalene
efg	-	Electric field gradient
S	-	Order parameter
S_{pq}	-	Order parameter which describes orientation in the pq direction
η	-	The asymmetry parameter, defined as: $\dfrac{S_{xx} - S_{yy}}{S_{zz}}$
k	-	Elastic force constant
STP	-	Standard temperature and pressure
C_{2v}^{*}	-	Includes C_{2v} and D_{2h} molecules

ACKNOWLEDGEMENT

To my sister

Mei-Leng

CHAPTER I

INTRODUCTION

I.   INTRODUCTION

The exact nature of the mechanisms of orientational order in the theory of liquid-crystalline systems is not fully understood.[1] An understanding of these physical interactions is of major importance in studies such as in the determination of the function of biological membranes, and the industrial use of liquid crystals as display devices. Such knowledge could also lead to a better understanding of intermolecular forces in the liquid phase.

Liquid crystal molecules are large and exist in many different conformations.[2] It was concluded that it would be difficult to obtain a better fundamental understanding from studies on these large molecules due to their flexibility. The logical starting point for a systematic investigation was to use small molecules dissolved in liquid crystal solvents.[3] The primary aims have been to understand (i) the orientational behaviour of the solutes and (ii) the intermolecular forces between solutes and the liquid crystal molecules responsible for this behaviour. In this thesis, an investigation of the interactions responsible for the orientation of small solutes in liquid crystalline systems is reported. The method used for the study of the anisotropic interactions of molecules dissolved in anisotropic solvents is nuclear magnetic resonance spectroscopy (NMR).

I.1   Liquid Crystalline Systems

I.1.1   Description

The first 'liquid crystalline' state was discovered by an Austrian botanist, Frederick Reinitzer in 1888.[4] He found that the compound he synthesized, cholestryl benzoate, appeared to have two melting points i.e. 145°C and 179°C. At 145°C, the solid melted to form a cloudy liquid which became clear at 179°C. In 1904, Lehman found that the cloudy intermediate was birefringent[5] and hence anisotropic, and he therefore suggested the name 'liquid crystal' for it. Since then, it has been found that one of every two hundred pure organic compounds exhibits the liquid crystalline state.

The liquid crystals referred to thus far are called thermotropics because they exhibit liquid crystallinity over a certain temperature range. Another major group is the lyotropic liquid crystals and these are formed by mixing two or more components. The best known examples of this group are aqueous soap solutions.

The properties of liquid crystals are intermediate between the liquid and solid state. These include the rotational and translational mobility of liquids and the optical properties of solids. The molecules in the liquid crystalline state have more order than those in the liquid state but less than those in the solid state.

The molecules that form thermotropic liquid crystals are generally elongated. These molecules usually contain benzene rings and often have strong dipoles towards their centres and weak dipoles towards their

ends. Due to intermolecular forces, these molecules tend to orient with their longest axes parallel to each other.

The thermotropic liquid crystals may be divided into three phases namely, nematic, cholestric and smectic.

Nematic phase - The nematic phase (Fig. I.1) has the lowest order of the three phases. This phase, if present always preceeds the transition to the isotropic liquid. The ordering consists of a preferred parallel arrangement of the long axes of large groups of molecules. In the absence of external forces, the preferred direction of the long axes of the molecules is not constant over large areas but varies continuously with position.
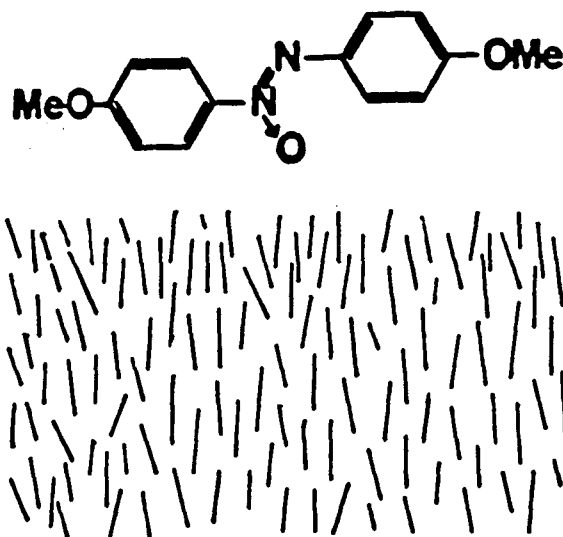
Fig. I.1: Arrangement of molecules in a nematic phase, e.g. 4-4'-dimethoxyazoxybenzene

Cholesteric phase - The cholesteric phase (Fig. I.2), regarded as a special case of the nematic phase, occurs only in optically active substances. It has a layered structure, and within the layers the molecules are oriented parallel to each other. The direction of the molecular axes in each layer is, however, slightly displaced with respect to adjacent layers, and the overall displacement follows a helical arrangement.

Smectic phase - For a given liquid crystal, this higher ordered phase (Fig. I.3) occurs at lower temperatures than the nematic and cholestric phases. The molecules are arranged in layers with their long axes parallel to each other.

I.1.2 Information obtainable from NMR Spectroscopy

In nuclear magnetic resonance experiments, the local magnetic fields at the nuclei, which determine the various transition frequencies, change with the orientation of the molecules relative to the external field. For solutes dissolved in isotropic solvents, there is rapid isotropic molecular motion. Consequently, dipolar and quadrupolar couplings and the anisotropy in the scalar couplings and chemical shifts which depend on orientation average to zero. Their NMR spectra are then governed by the average chemical shifts and indirect coupling constants between the nuclei.[6]
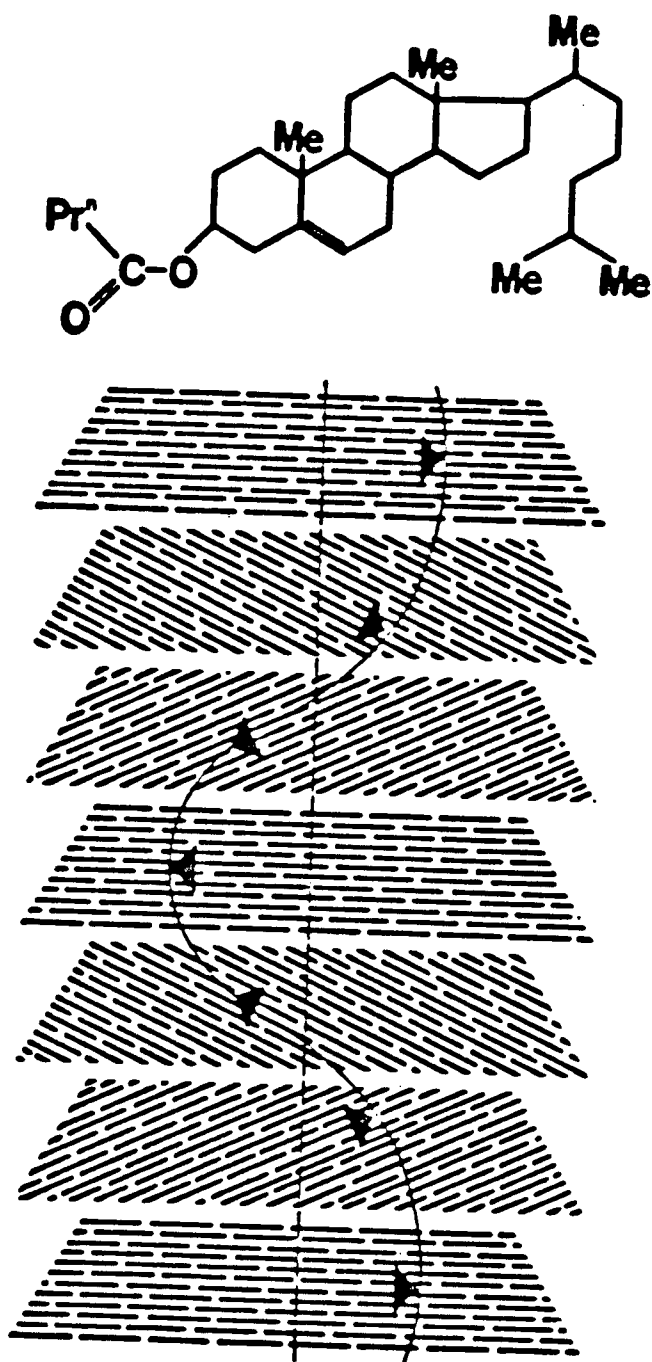
Fig. I.2: The molecular arrangement in a cholesteric mesophase, e.g. cholestryl propionate.
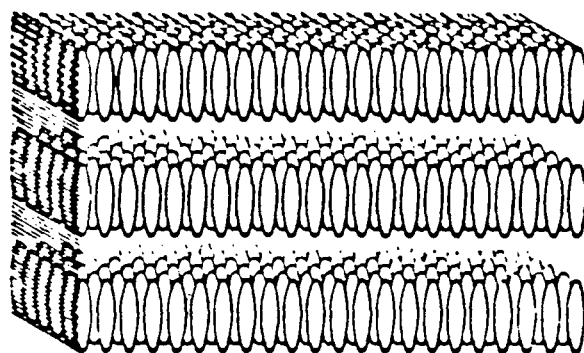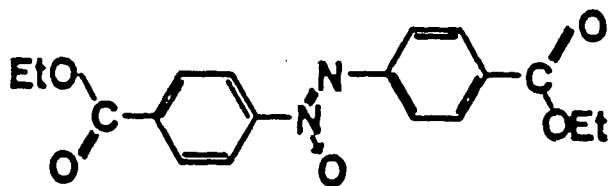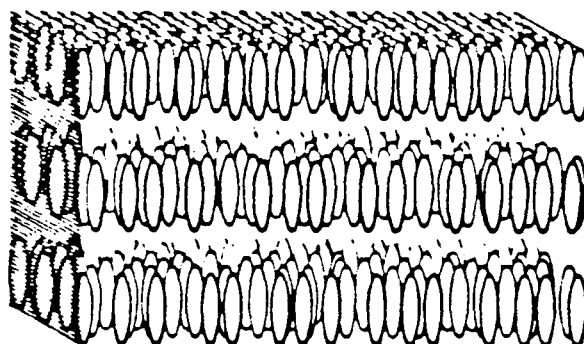
Fig. I.3   The structure of a smectic phase, e.g. 4-4'-diethyl-
            azoxybenzoate

For solutes in liquid crystalline solvents, the motion remains fast on the NMR time scale. However, due to the anisotropic environment of the molecules, different molecular orientations are no longer equally probable.[6] The NMR spectra are now weighted averages over all orientations. Important and useful information such as dipolar and quadrupolar couplings, and anisotropies in chemical shifts and indirect couplings can now be measured.

The nematic phase is most useful for examining the anisotropic properties of small solute molecules because it orients uniformly and easily in a magnetic field. The ^{1}H NMR spectrum of pure liquid crystals (in the nematic phase) is usually not resolved and has little observable fine structure. This is due to the large number of protons in the liquid crystals which gives rise to many energy levels. This multitude of energy levels produces many closely spaced transitions resulting in a spectrum which is a broad envelope. The ^{1}H NMR spectra of oriented solute molecules give relatively sharp lines and the direct dipole-dipole interaction is manifested by the fine structure in the spectrum. This spectrum is superimposed on that of the liquid crystal which is a broad, featureless background signal.

The spectrum of 2,4-hexadiyne, dissolved in the nematic phase of EBBA is as shown in Fig. I.4. The spectrum of the liquid crystal itself is broad and merges into the base line. The solute spectrum is well resolved in sharp lines, with a line width of 2 Hz which is typical of solutes in nematic phases.

The first NMR experiments of solutes oriented in liquid crystalline solvents were reported by Saupe and Englert in 1963.[7,8] Since then the
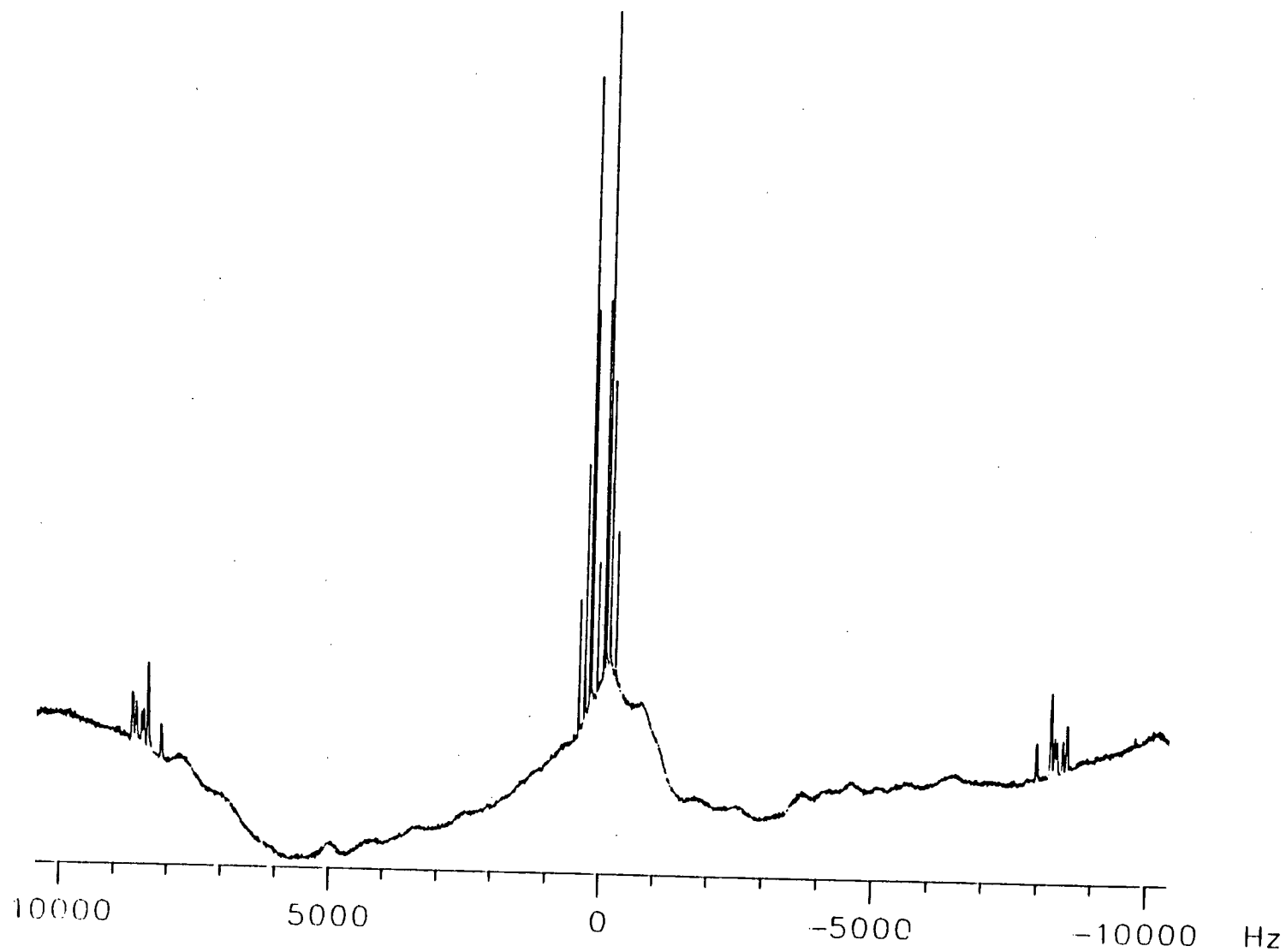
Fig. I.4 Proton NMR spectrum of 2,4-hexadiyne partially oriented in the liquid crystal EBBA

Hz axis labels: 10000, 5000, 0, -5000, -10000

NMR spectroscopy of oriented molecules has developed rapidly, the primary aim being the study of direct dipolar spin-spin couplings, which provide information on the molecular geometry of the solute.[9] This has resulted in the accumulation of a large body of structural data on different kinds of compounds dissolved in anisotropic phases. Despite the number of compounds which have been studied, the exact nature of the orientational mechanisms in liquid crystals is still not fully known.

I.1.3   Liquid Crystalline Systems - On the Orientational Order

Over the years, studies have led to several suggestions concerning the mechanism of solute orientation. These include dispersion forces,[10] size and shape,[11] and moments of inertia,[12,13] of the solutes. These models, however, do not adequately explain many experimental results.

In recent studies on methane[14-18] and hydrogen[3,14,19,20] and their deuterated analogs by Burnell et al., a better understanding of the mechanism of solute orientation has been achieved. In these studies, excellent agreement was obtained between the experimental and theoretical order parameters by assuming that the solvent-solute interaction is of second order tensorial form.

For hydrogen, the ratio of quadrupolar to dipolar coupling constants, B/D, should be a molecular property and this value should be the same as that measured in the gas phase by molecular beam magnetic resonance studies.[21] However, the ratios obtained[3] for HD and D_2 were

7% lower than expected for gas phase results. This suggests that the deuterons in the D_2 and HD were experiencing the presence of an external electric field gradient (efg) due to the liquid crystal environment. It was also suggested that the interaction between this electric field gradient and the molecular quadrupolar moment of the solutes accounts for most of the molecular orientation of hydrogen.[19]

The presence of this non-zero electric field gradient in these liquid crystals was further substantiated by experiments involving a series of deuterated methanes as solutes.[17] In these experiments, dipolar and quadrupolar coupling constants were measured. In the theoretical predictions of dipolar couplings, the interaction potential which describes the orientation of methane is of second order tensorial form.[16] This orientational mechanism involves the interaction of some liquid crystal mean field with the vibrationally induced anisotropy in some solute property. This interaction results in a coupling between vibration-rotation in the methane molecule which leads to a correct prediction of all the dipolar couplings.[16] This calculation involved three adjustable parameters. It was also shown that the deuteron quadrupolar couplings observed can be understood on the basis of the same vibration-rotation mechanism.[17] The calculation of these quadrupolar couplings, however, involves two additional molecular properties:

(i) the electric field gradient at the deuterium nucleus taken at equilibrium geometry, and

(ii) the derivative of this field gradient with respect to the C-D bond stretch.

The second parameter was found to be liquid crystal dependent. However, if the effect of the external field gradient as estimated from D_2 is taken into account, the variation in this parameter with liquid crystal disappears as is expected for a molecular property. This strongly suggests that methane and hydrogen experience the same field gradient.

In further experiments involving hydrogen, the external electric field gradient was found to be of opposite sign in EBBA and 1132; and it is a function of weight composition in mixtures of these two liquid crystals. It was experimentally shown that the average external field gradient experienced by a deuteron nucleus is zero in a 55 wt% 1132 mixture of 1132-EBBA at 301.4 ± 0.3 K. This mixture is useful because it provides a system for studying orientational order where the mechanism due to the electric field gradient is no longer present. The order parameter obtained from D_2 in this mixture was, however, not zero, but about 10% of the magnitude observed in each of the two component liquid crystals. This strongly indicates that there is an additional mechanism.

In a recent study by van der Est et al.,[22] a series of small molecules with C_{3v} or higher symmetry were dissolved in EBBA, 1132 and a 55 wt% 1132 mixture. A model was proposed by van der Est to describe the additional orientational mechanism. In the mixture where D_2 experiences zero efg, it was assumed that all the other solutes experience the same zero electric field gradient. The additional mechanism was proposed to be a short range hard body interaction between the solutes and solvent. This interaction is dependent on the dimensions of the solutes. It was shown that order parameters could be predicted

quite accurately using this model which is based on the size and shape of the solutes.

The order parameters were also calculated by using an interaction mechanism between the polarizability and the anisotropy of an electric field squared due to the liquid crystal. Again, good agreement between theoretical and experimental values was obtained, and this is not surprising since the polarizability is to a good approximation a function of the size and shape of the solute. In contrast the quadrupole moment is a function of the entire electronic structure and is not necessarily related to the size and shape of solutes. This suggests that if the contribution to the order parameter from the electric field gradient-molecular quadrupole moment interaction is removed, then any molecular property that is related to the size and shape can be used to predict orientations. In a sense, this poses a problem in that it is then difficult to distinguish between the different mechanisms. It is expected that for large solutes, however, the short range hard body interaction has to play an important role. Therefore, it seems worthwhile to investigate this mechanism in detail.

In the component liquid crystals, where an efg is present, two mechanisms, i.e. the electric field gradient-quadrupolar moment, and size and shape, were included in the prediction of order parameters. Again the parameters were quite accurately predicted. It was therefore concluded that the orientation of solutes in the liquid crystals can be described by these two mechanisms. The size and shape picture proposed by van der Est models well one of the orientational mechanisms in the series of C_3 molecules.

I.2 Objectives of this Thesis

The main objectives of the work presented here are two-fold:

(i) to study further the short range hard body interactions responsible for the orientation of solutes in the liquid crystal 55 wt% 1132, and

(ii) to test the effectiveness of the size and shape model which is used in the interpretation of the orientational order of the solutes.

For these purposes, a series of C_{2v} and D_{2h} molecules (hereafter referred to generally as C_{2v}^*) were chosen for the study. Two order parameters are required to describe fully the orientation of each C_{2v}^* solute. In C_{3v} molecules, only one parameter was involved. It is not clear whether each solute is oriented in exactly the same environment, hence comparison of order parameters of C_{3v} molecules is not quantitative. For C_{2v}^* molecules, quantitative comparison of parameters can be made because the two parameters of each solute describe orientation in exactly the same environment. For this reason, the series of C_{2v}^* molecules presents a more rigorous test for the model.

CHAPTER II

THEORY

II. THEORY

II.1   NMR of Partially Oriented Molecules

The theory of the NMR spectra of oriented molecules has been discussed by several authors.[9,23]

The Hamiltonian $\hat{H}$ of a system of spin $1/2$ nuclei in an isotropic medium is given by

$$\hat{H} = -\sum_i (1-\sigma_i)\, \nu_i \hat{I}_{Zi} + \sum_{i<j} J_{ij}\, \hat{I}_i \cdot \hat{I}_j \qquad [1]$$

where

σ_i is the chemical shift of nucleus i

ν_i is the resonance frequency of the bare nucleus i

$\hat{I}_i$ is the spin angular momentum operator of nucleus i

$\hat{I}_{Zi}$ is the component of the spin angular momentum of nucleus i in the Z-axis (of an external frame of reference).

J_{ij} is the isotropic indirect nuclear spin-spin coupling constant between nuclei i and j

The high resolution NMR spectrum is thus defined by the isotropic chemical shifts of the nuclei and the indirect nuclear spin-spin coupling constants between nuclei within the same molecule.

For a partially aligned spin system with the director of the nematic phase parallel to the external magnetic field, the Hamiltonian

is

$$\hat{H} = -\sum_i (1 - \sigma_{iZZ}) \nu_{iZ}\hat{I}_{Zi} + \sum_{i<j} J_{ij} \hat{I}_i \cdot \hat{I}_j$$
$$+ \sum_{i<j} D_{ij} (3 \hat{I}_{Zi} \hat{I}_{Zj} - \hat{I}_i \cdot \hat{I}_j) + \sum_i \frac{B_i}{3} (3\hat{I}_{Zi}^2 - \hat{I}_i^2) \qquad [2]$$

where

    D_{ij} is the direct spin-spin coupling between 2 spins

    B_i is the quadrupolar coupling constant of nucleus i

    σ_{iZZ} is the average ZZ component of the chemical shielding tensor

The anisotropies in indirect coupling constants can be neglected for protons.

For nuclei of spin greater than $1/2$ in a molecular fixed axially symmetric electric field gradient, -eq, the quadrupolar coupling is

$$B_i = \frac{3e^2qQ_i}{4h} S_i \qquad [3]$$

where

    eQ_i is the nuclear quadrupolar coupling constant

    S_i is the order parameter describing the average orientation of the direction associated with the symmetry axis of the electric field gradient tensor at nucleus i.

This equation applies for the case where internal and reorientational motions are separable. The observed quadrupole splitting, how-

ever, contains an extra contribution from the external electric field gradient of the liquid crystal. It can be written in the form:

$$B_{obs} = B_i - \frac{3eQ_i}{4h} F_{ZZ} \qquad [4]$$

where

F_{ZZ} is the external electric field gradient present in the liquid crystal.

The direct coupling D_{ij} is given by

$$D_{ij} = \frac{-h\gamma_i\gamma_j}{4\pi^2} < \frac{3 \cos^2\theta_{ij} - 1}{2 \; r_{ij}{}^3} > \qquad [5]$$

where

θ_{ij} is the angle between the magnetic field direction (Z-axis of the external frame of reference) and the axis connecting the 2 nuclei i and j separated by a distance r_{ij}

γ_i is the magnetogyric ratio of nucleus i

the angle brackets denote that the measured D_{ij} is averaged over all intermolecular and intramolecular motions.

$\frac{h\gamma_i\gamma_j}{4\pi^2}$ is equal to 120.067 kHz $Å^3$ for a pair of protons if r_{ij} is measured in $Å$ and D_{ij} in kHz.

If the intramolecular and intermolecular averages of equation [5] can be performed separately, one obtains

$$D_{ij} = -\frac{h\gamma_i\gamma_j}{4\pi^2} < \frac{1}{r^3_{ij}} > S_{ij} \qquad [6]$$

with the orientation parameter S_{ij} (the degree of orientation of the axis passing through i and j) defined as

$$S_{ij} = < \frac{3 \cos^2\theta_{ij} - 1}{2} > \qquad [7]$$

The average orientation of a rigid molecule of arbitrary symmetry in an anisotropic environment with cylindrical symmetry about the Z-axis of the external frame can be described by a 3x3 symmetric, traceless matrix (S) with 5 independent elements. The matrix elements are given by

$$S_{pq} = (1/2) < 3 \cos\theta_p \cos\theta_q - \delta_{pq} > \qquad [8]$$

where

p,q are the axes of a coordinate system xyz fixed within the molecule.

θ_p is the angle between the molecule p axis and the lab fixed Z-axis.

A molecule fixed direction a forming the angles α_x^a, α_y^a, α_z^a with the molecule-fixed xyz coordinate system has an S-value which is related to the matrix elements S_{pq} by the following equation

$$S_a = \sum_{p,q} \cos \alpha_p^a \cos \alpha_q^a \, S_{pq} \qquad [9]$$

This shows that given sufficient S_a values the matrix elements S_{pq} may be obtained and thus the ordering matrix $\{S\}$ for the molecule can be determined.

Since $\{S\}$ is symmetric and traceless, the 5 independent elements are related as follows:

$$S_{xx} + S_{yy} + S_{zz} = 0$$

and

$$S_{pq} = S_{qp} \qquad p,q = x,y,z \qquad [10]$$

For C_{2v}^* molecules, the number of independent S-values necessary for the description of orientation can be reduced from five to two by a suitable choice of molecular axes. If the C_2 axis is selected as the z-axis, and if x and y axes are chosen to be in the 2 perpendicular planes parallel to the z-axis, then $S_{xy} = S_{xz} = S_{yz} = 0$ and the two independent orientation parameters are S_{zz}, and $S_{xx}-S_{yy}$.

II.2 **Size and Shape Model [Ref. 22; van der Est, (private comm.)[24]]**

For a molecule in an axially symmetric environment, the components of the order parameter tensor can be calculated classically to be

$$S_{pq} = \frac{\int (3 \cos \theta_p \cos \theta_q - \delta_{pq}) \exp (-U(\Omega)/k_B T) \, d\Omega}{2 \int \exp (-U(\Omega)/k_B T) \, d\Omega} \qquad [11]$$

where the integration is over all orientations $\Omega = \Omega(\theta_p, \theta_q)$ and $U(\Omega)$ is the mean potential which describes the interaction between the solute molecule and the liquid crystal.

$U(\Omega)$ can be written as the sum of long and short range interactions

$$U(\Omega) = U_{SR}(\Omega) + U_{LR}(\Omega) \qquad [12]$$

where long range interactions involve intermolecular distances which are much larger than the molecular dimensions; and short range interactions involve those which are shorter than (or comparable to) the molecular dimensions.

The short range interaction consists of both an attractive and repulsive part as a function of the distance between the two interacting molecules. For short distances, the attractive part is ignored and the repulsive part becomes the dominant interaction.

The liquid crystal molecules are large and exist in many different conformations. An exact description of the interaction between these liquid crystal molecules and the solutes would be exceedingly compli- cated. The approach taken is to model the system in a simple but physically meaningful way.

The liquid crystal is modelled as an elastic tube parallel to the field direction. The solutes are assumed to be rigid and to fit into the system by stretching the tube. The walls of the tube are assumed to

be rigid such that any displacement is only in the X-Y direction, i.e. the energy to displace the wall in the Z-direction is negligible compared to the displacement energy in the X-Y direction. The stretched walls will then remain parallel to the Z-axis (Fig. II.1). The potential of the system is then effectively the energy needed to displace the tube upon the introduction of the solutes into the system. This displacement leads to a restoring force which is proportional to the deformation in the X-Y direction.

$$F(\Omega) \ = \ -k \int_{o}^{2\pi} r(\alpha,\Omega) \ d\alpha \ = \ -kc(\Omega) \qquad [13]$$

where

   $r(\alpha,\Omega)$ is the vector in the X-Y plane from the origin to the tube surface.

   α is the angle between the X-axis and $r(\alpha,\Omega)$.

   $c(\Omega)$ is the circumference of the deformed tube.

   k is the Hooke's law force constant.

The potential energy associated with the displacement of the liquid crystal tube in the X-Y direction is

$$U_{SR}(\Omega) \ = \ -\int F(\Omega) \ dc(\Omega) \ = \ \frac{kc^2(\Omega)}{2} \qquad [14]$$

$c(\Omega)$ is dependent on the model chosen to describe the size and
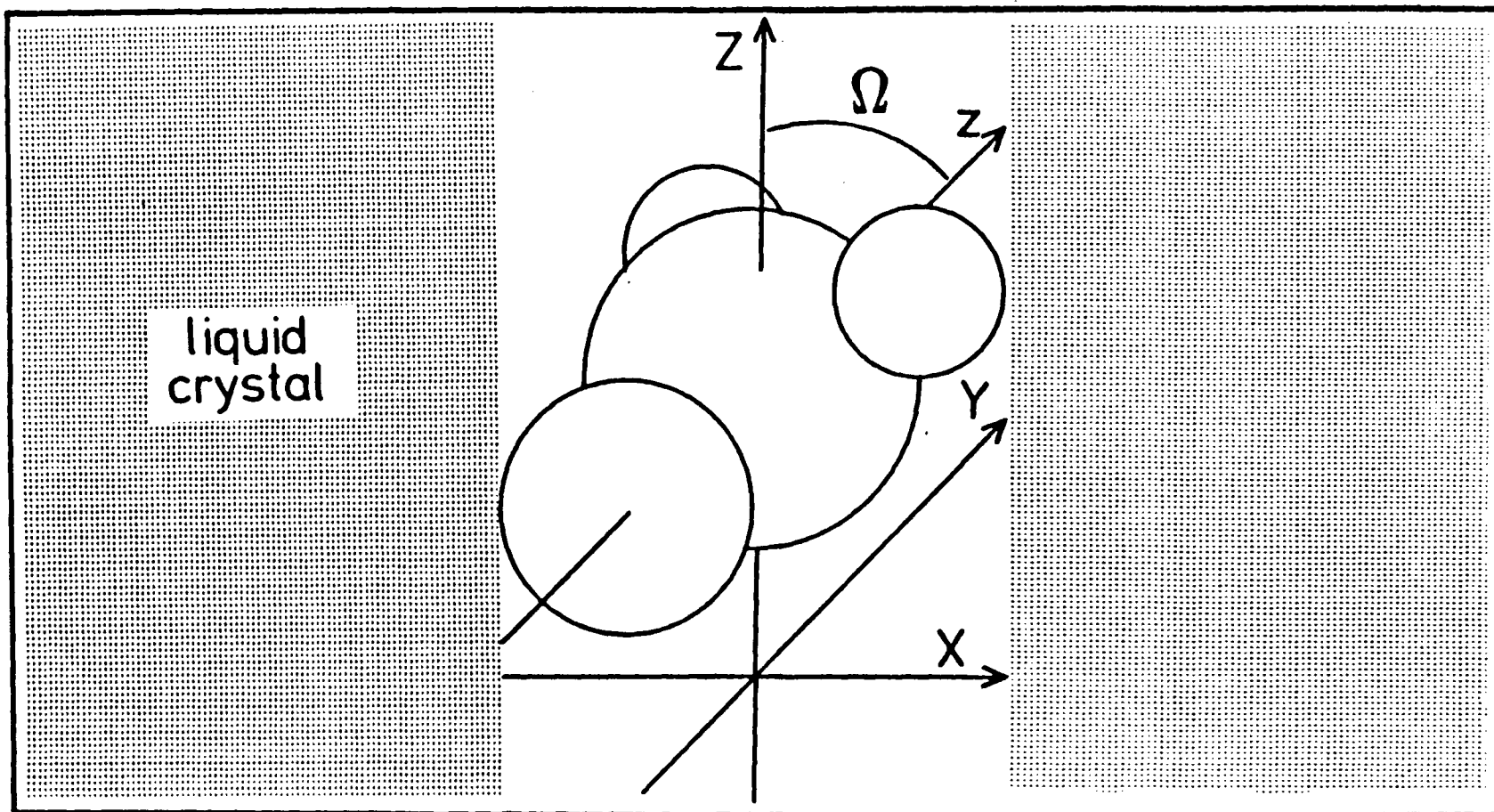
Fig. II.1   Elastic tube model for the short range interactions between
            solute and liquid crystal: The solute, represented by an
            array of van der Waals spheres displaces the liquid
            crystals. The displaced volume is a tube with its wall
            parallel to the laboratory fixed Z-axis. Ω is the angle
            between the molecule and liquid crystal axes

shape of the solute molecules. This circumference is also the surface of the elastic tube which interacts with the solute molecules. This surface acts as a boundary in separating the molecules from a region which is inaccessible to these solutes. The inaccessible region is not well-defined and as such the surface has to be calculated differently for each solute. To overcome this difficulty, it is assumed that the surfaces of the elastic tube and the solute molecules are hard, so $c(\Omega)$ is taken to be the circumference of the projected molecule in the X-Y plane.

The solute molecule is modelled as a collection of van der Waals spheres centred on fixed positions (x_i, y_i, z_i) in the molecular axis system. Each atom has a sphere of radius r_i associated with it, r_i is the van der Waals radius for the atom. The projection of the molecule from the molecule fixed axis onto the space fixed axis is done by two rotations of the axis system. The first rotation is in a counter-clockwise direction through an angle θ about the space fixed Y axis. This is followed by a second rotation in a counter clockwise direction through an angle ϕ about the resulting z-axis. The coordinates of the ith atom of the solute molecule in the X-Y plane are given by

$$X_i = x_i \cos\theta \cos\phi - y_i \cos\theta \sin\phi + z_i \sin\theta \qquad [15]$$
$$Y_i = x_i \sin\phi + y_i \cos\phi$$

Thus the projection of the molecule in the X-Y plane is an array of overlapping circles centred at (X_i, Y_i) (Fig. II.2.A). The ith projected circle can be described by

$$(X-X_i)^2 + (Y-Y_i)^2 = r_i^2$$

The maximum and minimum values of X and Y of the ith projected atom are given by

$$Xmax_i = X_i + r_i$$
$$Xmin_i = X_i - r_i$$
$$Ymax_i = Y_i + r_i$$
$$Ymin_i = Y_i - r_i$$

If $Xmin_k$ and $Ymin_j$ are the smallest, and $Xmax_l$ and $Ymax_m$ are the largest of the coordinates, then the points $(Xmax_l, Y_l)$, $(Xmin_k, Y_k)$, $(X_j, Ymin_j)$ and $(X_m, Ymax_m)$ lie on the outer surface of the projected circles.

The perimeter of the projected molecule is determined using the minimum circumference of the array of the overlapping circles, which is defined in the same manner for all solute molecules (Fig. II.2.B). $U(\Omega)$ can then be calculated from equation [14] using $c(\Omega)$. The order parameters can then be obtained by an integration of equation [11] over all orientations of the solute. For molecules with symmetry C_{2v}^*, there are two independent parameters S_{zz} and S_{xx}.

In terms of the model,

$$S_{zz} = \frac{\int_o^\pi \int_o^{2\pi} (3 \cos^2 \theta - 1) \exp \{(-kc^2(\theta,\phi)/2k_BT\} \sin \theta \; d\theta d\phi}{2\int_o^\pi \int_o^{\pi/2} \exp \{ -kc^2(\theta,\phi)/2k_BT\} \sin \theta \; d\theta \; d\phi}$$

$$S_{xx} = \frac{\int_o^\pi \int_o^{2\pi} (3 \sin^2 \theta \cos^2 \phi - 1) \exp \{(-kc^2(\theta,\phi)/2k_BT\} \sin \theta \; d\theta d\phi}{2\int_o^\pi \int_o^{\pi/2} \exp \{ -kc^2(\theta,\phi)/2k_BT\} \sin \theta \; d\theta \; d\phi} \qquad [17]$$

The single parameter of the model, the force constant k, is obtained by a least squares procedure where there was optimal agreement between the theoretical and the experimental order parameters of the series of solutes in the same liquid crystal.
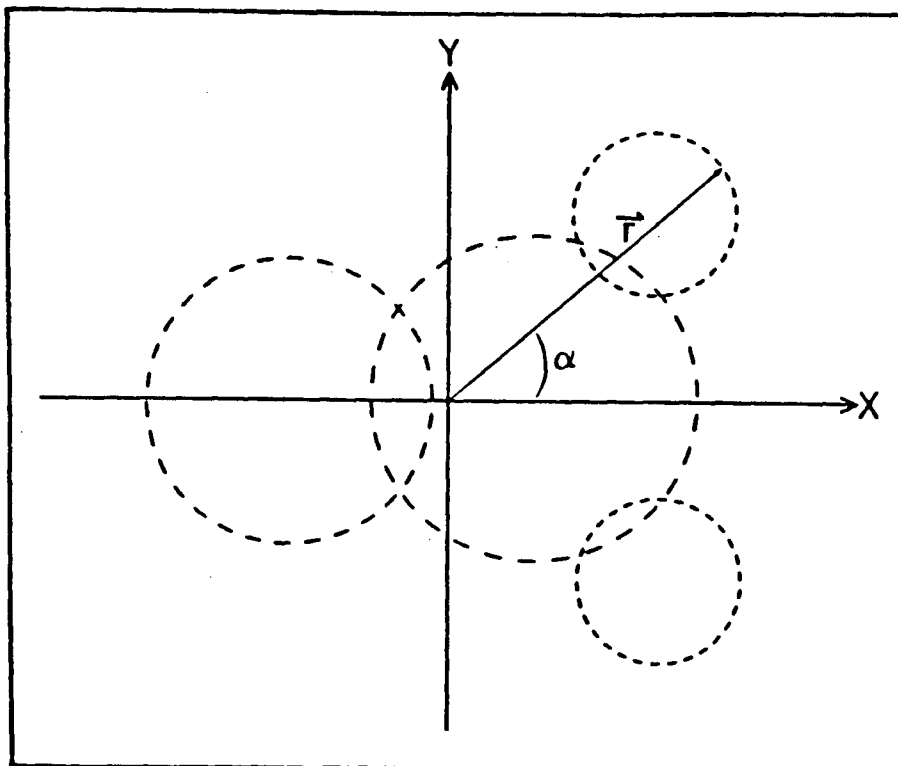
Fig. II.2   Projection of solute in X-Y plane:
A: r is a vector from the origin to the surface of the pro-
jected molecule and α is the angle between r and the x-axis.
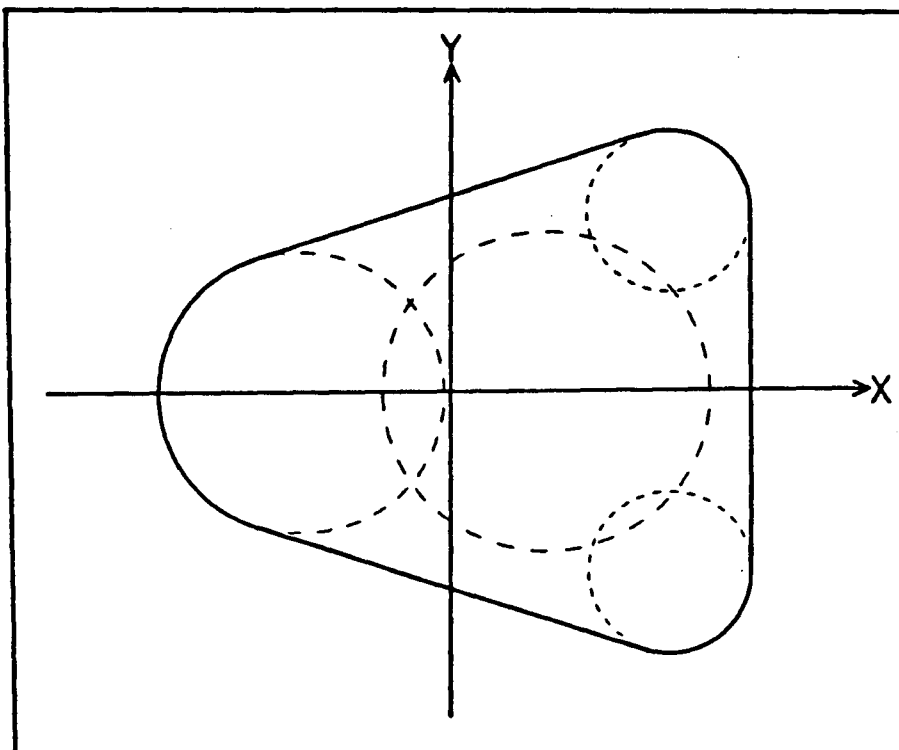
Fig. II.2   Projection of solute in X-Y plane:
B: The minimum circumference of the elastic tube represent-
ing the deformation of the liquid crystal solvent by a
solute at some orientation is shown in bold face.

CHAPTER III

EXPERIMENTAL
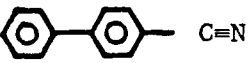
III. EXPERIMENTAL

The liquid crystals used were deuterated EBBA: N-(4-ethoxybenzyli-dene)-2,6-dideutero-4-n-butylaniline and 1132: Merck ZLI 1132. The compounds listed in Table IV.1 were purchased from a variety of chemical suppliers.   These compounds and 1132 were used without further purifi-cation. The composition of 1132 is given as follows:[25]

Merck Licrystal ZLI 1132:   24% $C_{16}H_{21}N$ (I)

36% $C_{18}H_{25}N$ (II)

25% $C_{20}H_{29}N$ (III)

15% $C_{24}H_{29}N$ (IV)

where
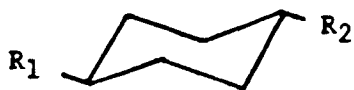
I   : R_1 — C_3H_7 R_2 — Ph-C≡N

II : R_1 — C_5H_{11} R_2 — Ph-C≡N

III : R_1 — C_7H_{15} R_2 — Ph-C≡N

IV : R_1 — C_5H_{11} R_2 —   C≡N

The deuterated EBBA was synthesized as in Section III.1. and III.2.

III.1   Deuteration of 4-n-butylaniline

The selective deuteration of 4-n-butylaniline at two ring positions
is as illustrated below:[26]
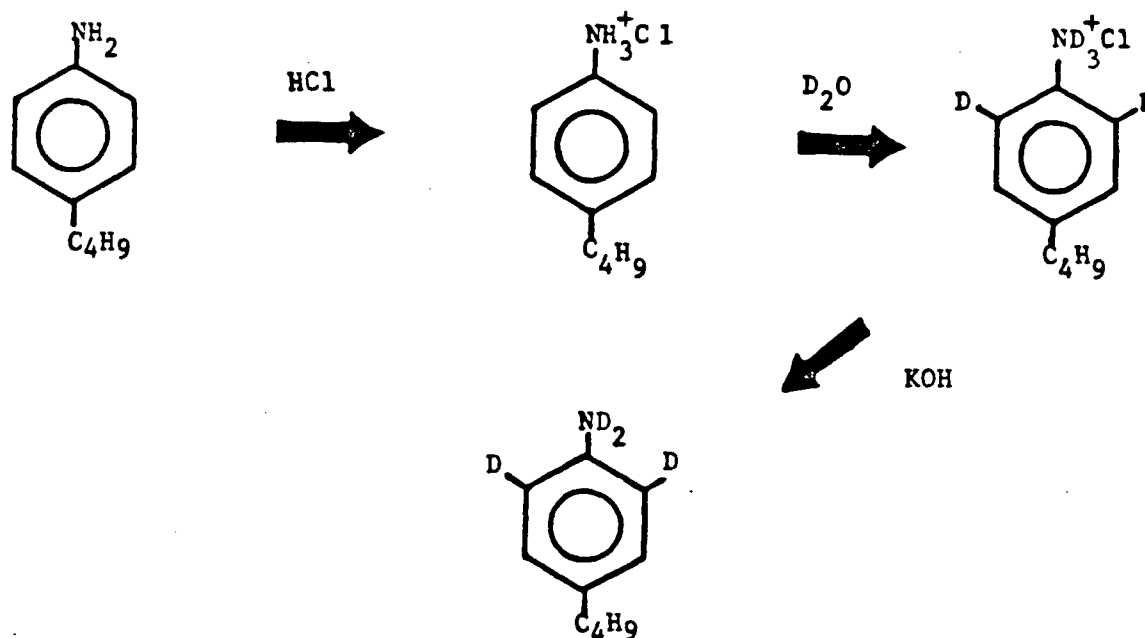
4-n-Butylaniline was first purified by vacuum distillation to give
a clear liquid. 100 g of this was then added dropwise to ~350 ml of 2M
HCl. The amine salt that formed was soluble in water, and gave a
yellowish oily solution. Water was removed by evaporation.   This was
followed by the addition of ~100 ml D_2O to dissolve the salt. The
mixture was then refluxed for 3 hours to deuterate the two ring posi-
tions.   The   excess acid was then neutralized with KOH. N,N,2,6-tetra-
deutero-4-n-butylaniline was extracted with ether and further purified
by vacuum distillation.

III.2   Preparation of EBBA

EBBA was prepared by the reaction as illustrated below:[27]
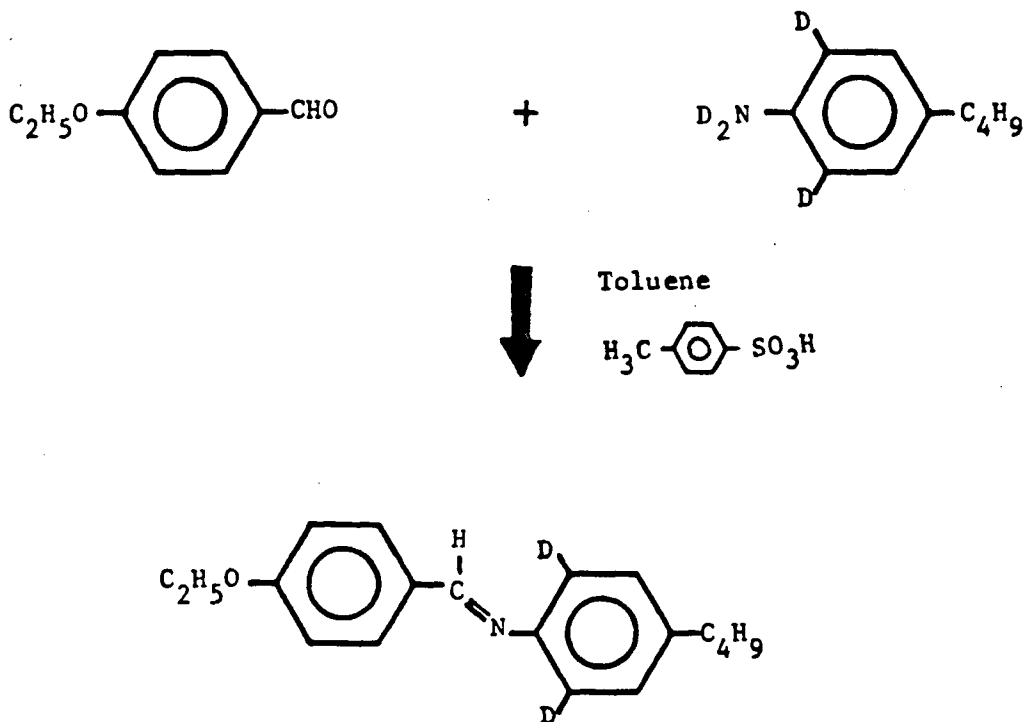
60 g of deuterated 4-n-butylaniline, 60 g of 4-ethoxybenzaldehyde
(both purified by vacuum distillation), and 0.75 g of 4-toluenesulfonic
acid were dissolved in 600 ml of toluene and refluxed for 4 hours. The
water formed during the reaction was removed azeotropically by means of
a Dean Stark apparatus. At the end of the reaction, toluene was removed
by evaporation to yield a dark brown liquid. The compound was recrys-
tallized from methanol until constant phase transition temperatures were
obtained. The pale yellow flaky crystals of EBBA were left to dry under
vacuum overnight.   Transition points obtained for the purified EBBA
were: 308 ± 1K and 351 ± 1K. These temperatures agree well with the

literature values[*].[28]

$$\text{Crystals} \xrightarrow[(308K)^*]{308K} \text{Nematic Phase} \xrightarrow[(351K)^*]{352K} \text{Isotropic Phase}$$
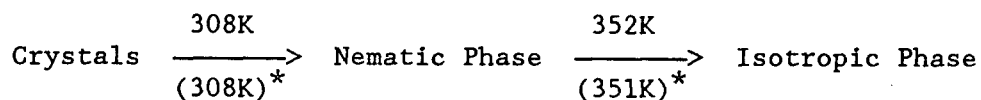
The deuteron NMR spectrum of EBBA showed two doublets of line width 600 Hz and splittings of 22 and 19 kHz. The high resolution proton NMR spectrum showed that the compound is pure.

III.3   Preparation of 55 wt% 1132 mixture

13.5 g of EBBA and 16.5 g of 1132 in a 50 ml Erlenmeyer flask were mixed by heating the mixture to the isotropic phase and vortexing it. This process was repeated several times. The mixture was stored under nitrogen and in the dark to prevent any degradation of the compounds.

A high pressure sample of D_2 in this mixture was made up (see Section III.4) to check the magnitude of the average electric field gradient. F_{ZZ} was found to be $0.227 \pm 0.79 \times 10^{10}$ esu in this 55 wt % 1132 mixture of 1132-EBBA at 301.4 K (see Section III.5). This value is zero within the error limits.

III.4   Preparation of NMR Samples

The 55 wt % 1132 mixture of 1132-EBBA liquid crystal in 5 mm sample

tubes was first thoroughly degassed by the freeze-pump-thaw method. For solutes which are liquids or solids, a sufficient amount of the compound was added to the liquid crystal mixture to produce a concentration of 1 mole percent. The tubes were then capped and thoroughly mixed by vortexing the samples in the isotropic phase. Samples of furan and thiophene in 1132 and EBBA were made up in a similar manner. For the D_2 sample, a sufficient volume of the gas to produce a pressure of 25 atm under STP conditions was condensed into the liquid crystal mixture in a constricted 9 mm tube cooled in liquid helium. The tube was then sealed and pressure tested in an oven at about 425 K. All samples were stored in the dark to prevent degradation of EBBA.

III.5   NMR Spectroscopy

Proton and deuteron spectra were obtained using Fourier Transform techniques with a Bruker WH-400 NMR spectrometer equipped with an Oxford Instruments 9.4T superconducting magnet, operating at 400.1 MHz for protons and 61.4 MHz for deuterons. The deuteron signal of the deuterated EBBA was observed through the lock channel thus ensuring identical conditions. The temperature was controlled by means of a variable temperature gas flow unit and calibrated using the proton chemical shift differences from a sample of ethylene glycol. The dial temperature of 304 K was calibrated to 301.4 ± 0.3 K. Other temperatures were not corrected. All samples were heated up to the isotropic phase and vortexed before being placed in the probe. Samples were usually left to

equilibrate for half an hour before nmr spectral acquisition. All experiments were done without field frequency lock. It was therefore important to obtain the spectra in the shortest time possible to counteract magnetic field drift and slight temperature fluctuations.

A pulse width of 12 μs was used for all the proton experiments. The number of scans used varied from 8 to 32 and the line width was in the range of 2-10 Hz depending on the samples. For the deuteron spectra, a pulse width of 10 μs and a relaxation delay of 0.3 s were used. A thousand scans were necessary to obtain a good signal to noise spectrum.

Solutes in 55 wt % 1132 - The spectra of all the solutes in 55 wt% 1132 were obtained at 301.4 K (dial T = 304 K). For each sample, a proton spectrum of the solute and a deuteron spectrum of the liquid crystal were collected.

D_2 in 55 wt % 1132 - Deuteron spectra of both the solute and the deuterated EBBA were obtained at various temperatures between 304-325 K (dial T).

Furan and thiophene - Samples of furan and thiophene in 55 wt % 1132 mixture were also studied as a function of temperature ranging from 304-325 K (dial T). At higher temperatures, the presence of temperature gradients along the sample tube caused line broadening in the spectra. This could be slightly reduced by increasing the air flow of the heater. Proton spectra of furan and of thiophene in the liquid crystals 1132 and

EBBA were collected at 301.4 K.

III.6   Spectral Analysis

Proton spectra of solutes - The proton spectra obtained were then analyzed using the iterative programs LEQUOR[29] and SHAPE.[30] For each compound, a set of starting parameters of chemical shifts, indirect coupling constants, order parameters and an appropriate geometry from electron diffraction or microwave studies, were fed into the program LEQUOR. Iterative assignment procedures were used until all the peaks in the calculated spectrum were assigned and the root mean square (rms) error between calculated and experimental peaks was of the order of the digital resolution of the experimental spectrum. The anisotropic chemical shifts, indirect coupling constants and dipolar coupling constants, (D_{ij}) were obtained from the final spectral calculations. The D_{ij} values were then used as input into the program SHAPE to give the molecular order parameters S_{pq} as well as a refined geometry.

Deuteron spectra of D_2 in 55 wt % 1132 - The deuteron NMR spectrum is as shown in Fig. III.1. The spectral analysis yielded values of B_i and D_{ij}. The value of D_{ij}, in conjunction with the vibrationally averaged value of r^{-3}, was then used to obtain the value of the order parameter from equation [6]. An experimental value of the electric field gradient, F_{ZZ}, was then obtained from equation [4].
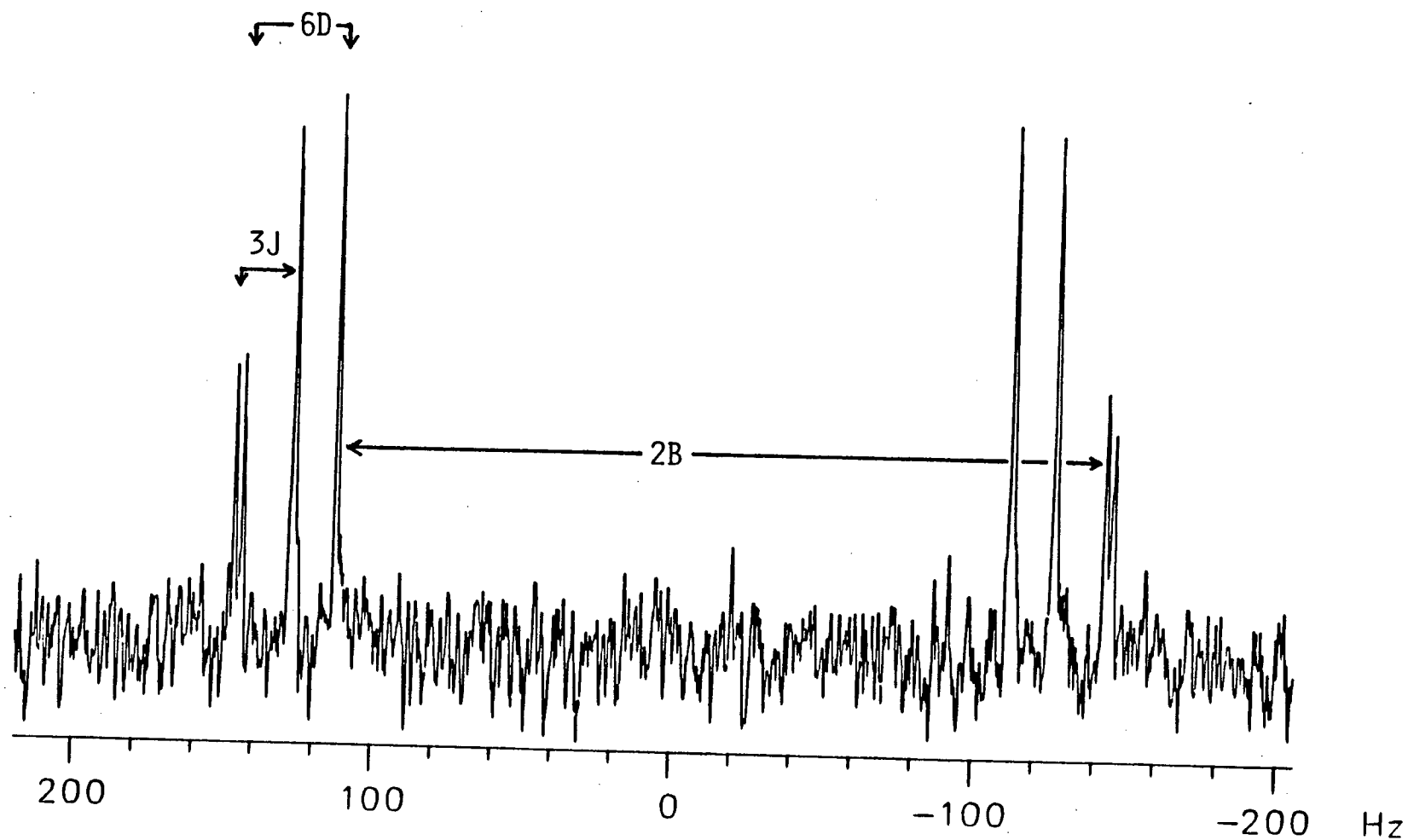
Fig. III.1   Deuteron NMR spectrum of D_2 partially oriented in the
liquid crystal 55 wt% 1132 mixture at 301.4 K

Deuteron spectra of deuterated EBBA - The quadrupolar splittings of the deuterated EBBA were obtained by measuring the distance (Hz) between the two doublets.

CHAPTER IV

RESULTS

IV.   RESULTS

IV.1   Solutes in 55 wt% 1132 mixture at 301.4K

Examples of the high resolution proton NMR spectra of a solute dissolved in the nematic liquid crystal 55 wt% 1132 mixture are as shown in Figs. IV.1.A and IV.2.A. Fig. IV.1.A is the spectrum of 1,4-dibromobenzene in the liquid crystal mixture. It has a line width of 5 Hz, spectral width of ~9,000 Hz and consists of twelve peaks. The spectrum is simple and symmetrical because the molecule is a four spin AA'A''A''' system. Fig. IV.2.A is the spectrum of partially oriented fluorobenzene with a line width of 2 Hz, spectral width of 3500 Hz and has over seventy peaks. Since the molecule is a six spin AA'BB'CX system, the resulting spectrum is complicated.

An example of the deuteron spectrum of deuterated EBBA in the 55 wt% 1132 is as given in Fig. IV.3. The quadrupolar splittings of the outer and inner doublets are about 19 and 16 kHz respectively, and the line width is about 600 Hz.

The experimental proton spectra were analyzed using the program LEQUOR as described earlier (Section III.6). The spectra simulated by this program are shown in Figs. IV.1.B and IV.2.B.

From the spectral analyses, direct dipolar coupling constants, indirect coupling constants, chemical shift differences and the rms errors of the fits were obtained and these are summarized in Table IV.1.

(A)

(B)

| -695 00 | -540.55 | -386 11 | -231.67 | -77 22 | 77.22 | 231.67 | 386 11 |

• 10¹
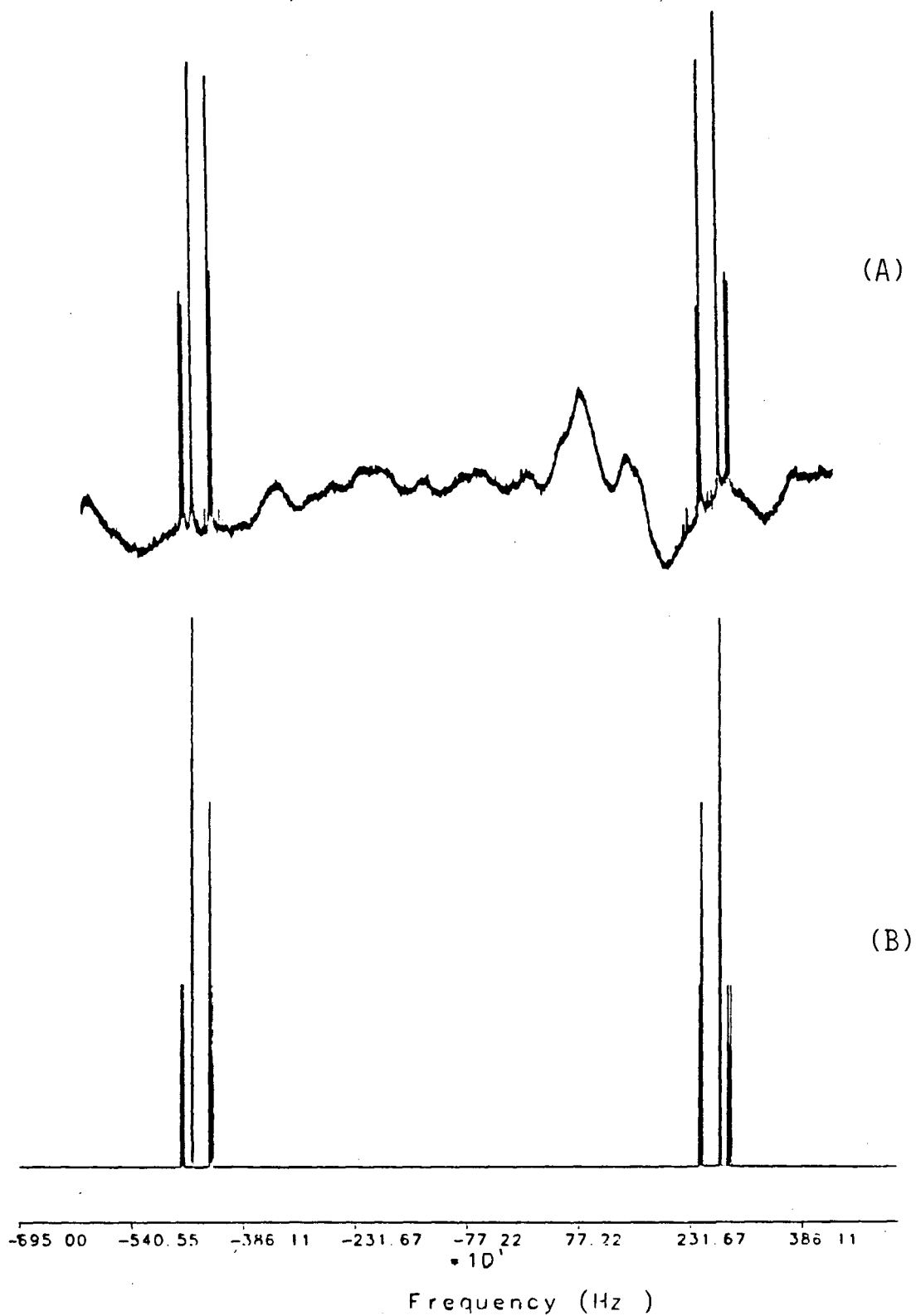
Frequency (Hz)

Fig. IV.1   Proton NMR spectrum of 1,4-dibromobenzene partially
            oriented in 55 wt% 1132: (A) experimental (B) computer
            simulation.   Temperature = 301.4 K.   Concentration = 1
            mole %.   Spectrometer Frequency = 400 MHz.
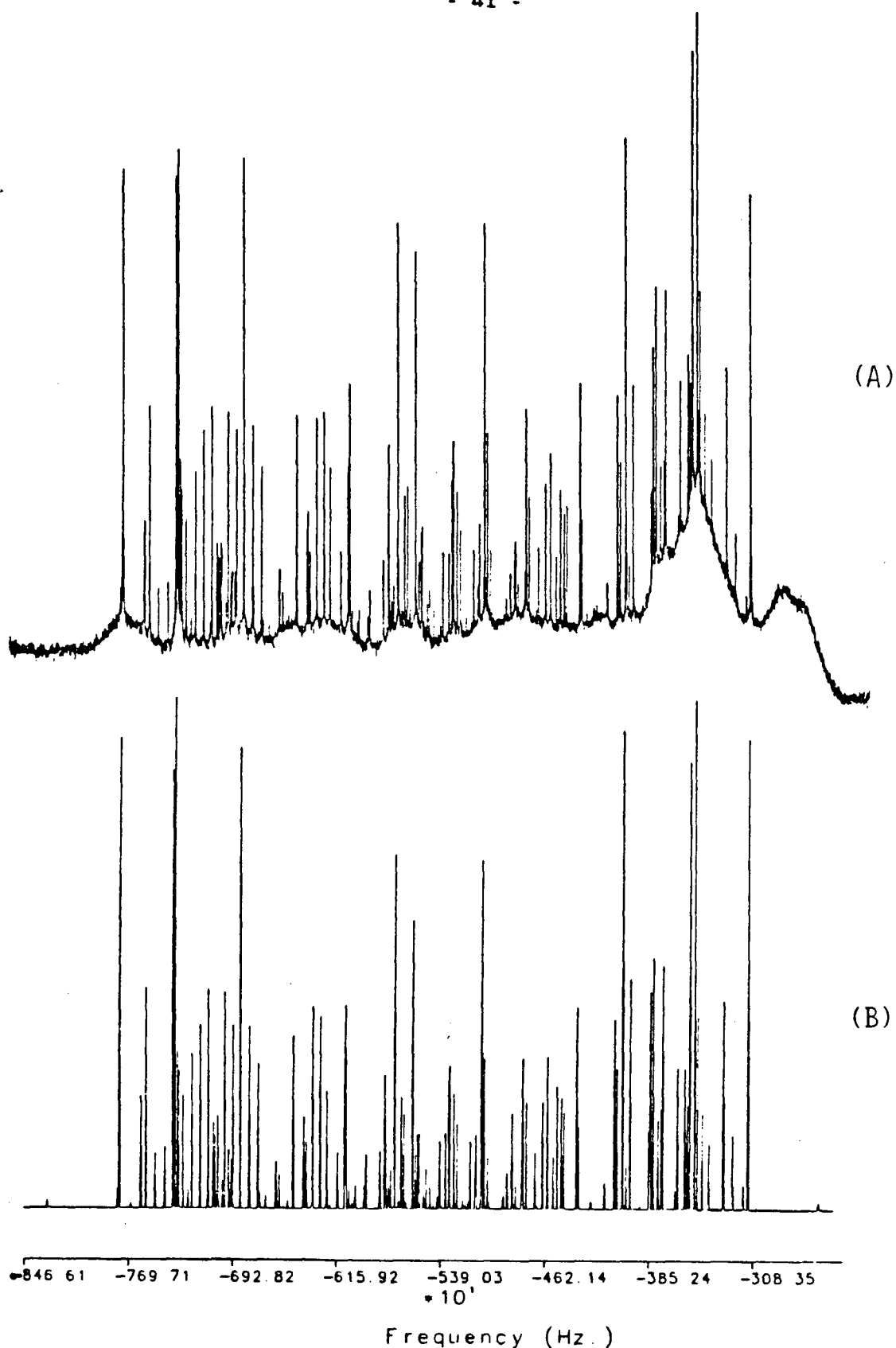
Fig. IV.2   Proton NMR spectrum of fluorobenzene partially oriented in
55 wt% 1132: (A) experimental (B) computer simulation.
Temperature = 301.4 K.   Concentration = 1 mole %.
Spectrometer Frequency = 400 MHz.
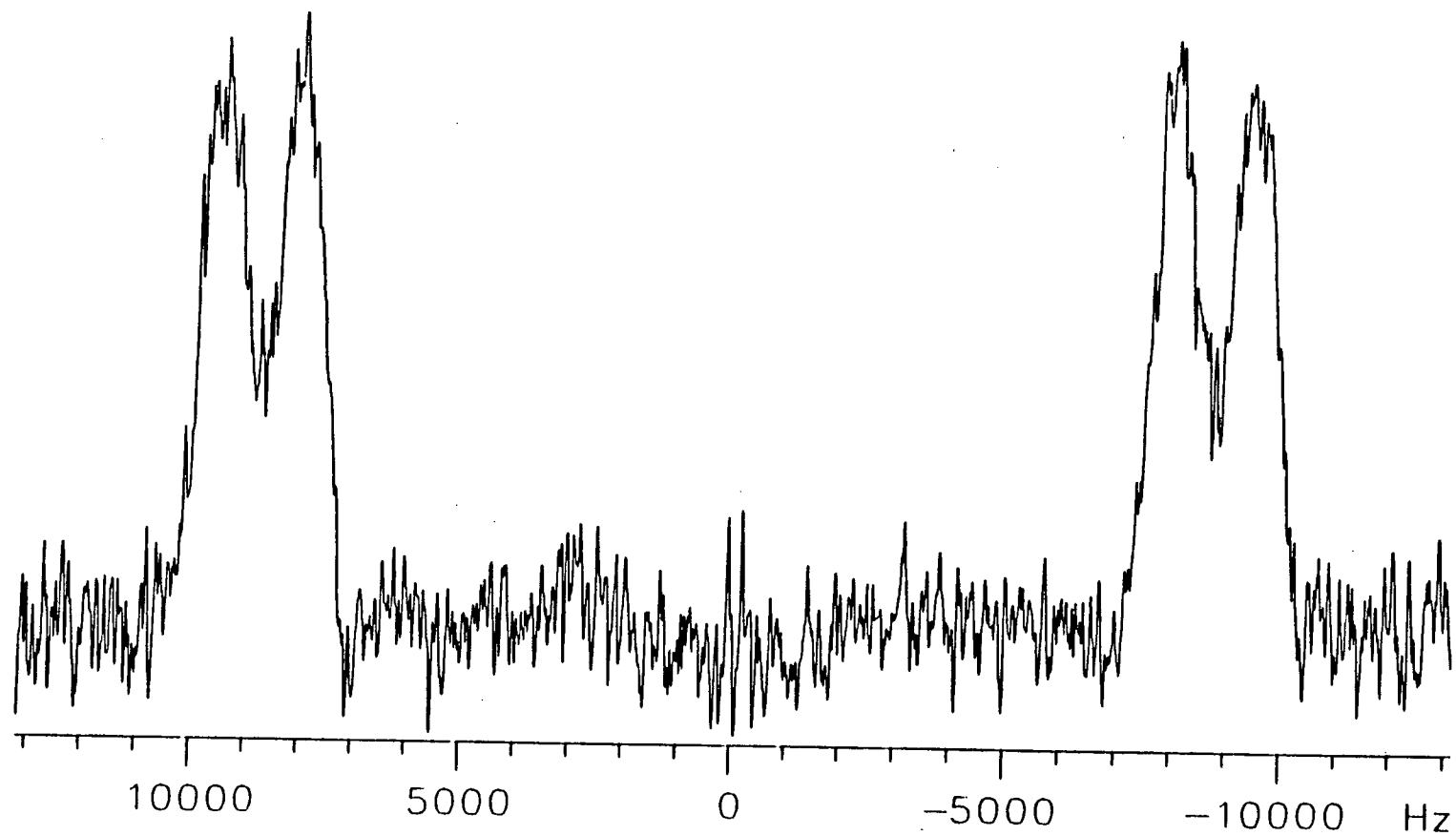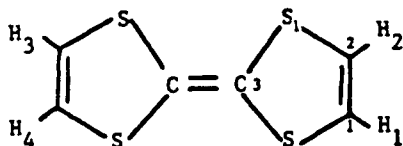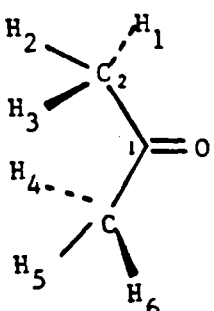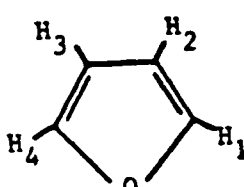
Fig. IV.3   Deuteron NMR spectrum of deuterated EBBA at 301.4 K

Table IV.1: Experimental dipolar couplings[a] (Hz), indirect couplings[b] (Hz), chemical shift differences (Hz), and the rms errors[c] (Hz) obtained from the program LEQUOR for solutes dissolved in the nematic liquid crystal 55 wt% 1132 at 301.4 K.

Molecule	Parameter		References[d]
1 TTF (tetrathiofulvalene)	D_{12}	-674.42 (5)[e]	31
	D_{13}	68.95 (6)	
	D_{14}	90.06 (6)	
	J_{12}	8.00	
	rms	0.20	
2 Acetone	D_{12}	569.48 (3)	32
	D_{14}	-171.68 (3)	
	J_{14}	0.55	
	rms	0.36	
3 Furan	D_{12}	-292.80 (4)	33
	D_{13}	-110.91 (4)	
	D_{14}	-158.85 (4)	
	D_{23}	-524.61 (5)	
	J_{12}	1.75	
	J_{13}	0.81	
	D_{14}	1.48	
	J_{23}	3.27	
	$\nu_2 - \nu_1$	371.56 (9)	
	rms	0.13	

4   Thiophene
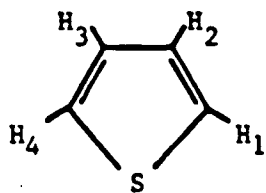
D_{12}	-549.56 (5)	34
D_{13}	- 99.16 (6)	
D_{14}	- 75.22 (10)	
D_{23}	-379.93 (9)	
J_{12}	4.90	
J_{13}	1.04	
J_{14}	2.84	
J_{23}	3.50	
$\nu_2 - \nu_1$	84.80 (15)	
rms	0.21	
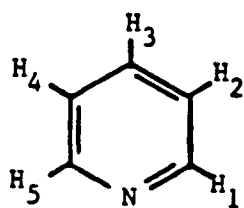
5   Pyridine

D_{12}	-368.7 (4)	35
D_{13}	- 93.7 (4)	
D_{14}	- 96.6 (4)	
D_{15}	-189.2 (6)	
D_{23}	-703.4 (3)	
D_{24}	-164.8 (8)	
J_{12}	4.86	
J_{13}	1.85	
J_{14}	0.98	
J_{15}	-0.13	
J_{23}	7.66	
J_{24}	1.36	
$\nu_2 - \nu_1$	539 (1)	
$\nu_2 - \nu_3$	103 (1)	
rms	1.3	

6   2,6-Difluoropyridine
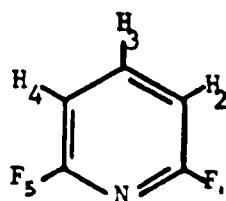
D_{12} -247.77 (11)   36

D_{13} - 84.35 (11)

D_{14} -103.84 (10)

D_{15} -179.2 (3)

D_{23} -903.66 (6)

D_{24} -222.50 (16)

J_{12} - 2.47

J_{13} 7.97

J_{14} 1.19

J_{15} - 12.23

J_{23} 7.94

J_{24} 0.55

$\nu_2 - \nu_3$ 404.5 (3)

rms   0.42

7   Fluorobenzene
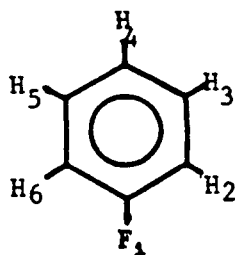
D_{12} -509.84 (7)   37

D_{13} -148.78 (7)

D_{14} -113.33 (4)

D_{23} -1067.95 (3)

D_{24} -176.05 (5)

D_{25} - 71.60 (3)

D_{26} - 76.30 (5)

D_{34} -562.49 (5)

D_{35} - 75.67 (5)

J_{12} 8.90

J_{13} 5.57

J_{14}	0.20	
J_{23}	8.35	
J_{24}	1.03	
J_{25}	0.40	
J_{26}	2.58	
J_{34}	7.50	
J_{35}	1.76	
$\nu_2 - \nu_3$	87.9	(1)
$\nu_2 - \nu_4$	63.9	(1)
rms	0.22	

8 Chlorobenzene
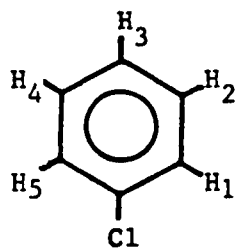
D_{12}	-1578.04	(9)	38
D_{13}	-232.1	(3)	
D_{14}	- 55.29	(9)	
D_{15}	- 10.4	(5)	
D_{23}	-430.7	(3)	
D_{24}	- 10.5	(5)	
J_{12}	8.15		
J_{13}	1.14		
J_{14}	0.50		
J_{15}	2.24		
J_{23}	7.57		
J_{24}	1.71		
$\nu_2 - \nu_1$	8	(1)	
$\nu_2 - \nu_3$	100.1	(5)	
rms	0.49		

9   Iodobenzene
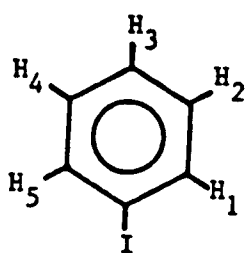
D_{12}	-1886.73	(12)
D_{13}	-260	(1)
D_{14}	- 39.82	(13)
D_{15}	39	(3)
D_{23}	-312	(1)
D_{24}	38	(3)
J_{12}	7.93	
J_{13}	1.12	
J_{14}	0.47	
J_{15}	1.88	
J_{23}	7.50	
J_{24}	1.74	
$\nu_2 - \nu_1$	52	(7)
$\nu_2 - \nu_3$	232	(4)
rms	0.69	

38

10   1,2-Dichlorobenzene
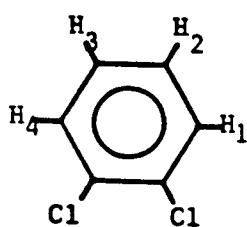
D_{12}	-1060.41	(6)
D_{13}	-135.72	(8)
D_{14}	- 66.27	(16)
D_{23}	-508.42	(16)
J_{12}	8.06	
J_{13}	1.54	
J_{14}	0.31	
J_{23}	7.48	
$\nu_1 - \nu_2$	59.7	(3)
rms	0.29	

39

11   1,2-Dicyanobenzene
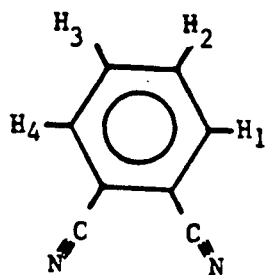
D_{12} -1213.22 (17)   40

D_{13} -144.65 (19)

D_{14} - 64.9 (4)

D_{23} -499.7 (4)

J_{12} 7.90

J_{13} 1.26

J_{14} 0.61

J_{23} 7.81

$\nu_2 - \nu_1$ 87   (1)

rms   0.64

12   1,3-Dichlorobenzene
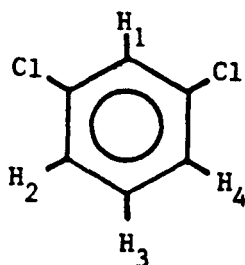
D_{12} -107.00 (9)   41

D_{13} - 28.12 (14)

D_{23} -1207.88 (7)

D_{24} -296.89 (17)

J_{12} 1.97

J_{13} 0.36

J_{23} 8.10

J_{24} 0.89

$\nu_1 - \nu_2$ 261.0   (3)

$\nu_1 - \nu_3$ 186.7   (3)

rms   0.37

13   1,3-Dinitrobenzene

D_{12} -133.6 (6)   42

D_{13} - 38   (1)

D_{23} -1431.0 (4)
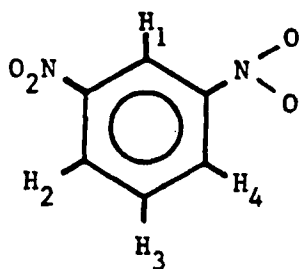
D_{24}	-355	(1)
J_{12}	2.20	
J_{13}	0.50	
J_{23}	8.30	
J_{24}	2.00	
$\nu_3-\nu_1$	531	(2)
$\nu_2-\nu_1$	443	(2)
rms	1.90	

14 1,4-Dichlorobenzene
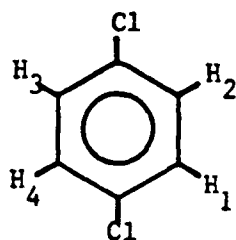
D_{12}	-2419.38	(10)	43
D_{13}	- 25.43	(13)	
D_{14}	-107.04	(13)	
J_{12}	8.55		
J_{13}	0.39		
J_{14}	2.58		
rms	0.44		

15 1,4-Dibromobenzene
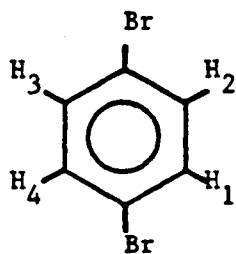
D_{12}	-2727.87	(10)	44
D_{13}	- 12.34	(12)	
D_{14}	-150.86	(11)	
J_{12}	8.41		
J_{13}	0.46		
J_{14}	2.38		
rms	0.40		

a   The numbering of the protons is as shown in the drawings.

b   Indirect coupling constants were obtained from the literature.

c   This is the rms error of the fit of the experimental spectra to the calculated spectra by the program LEQUOR.

d   References for indirect coupling constants.

e   Numbers in brackets refer to errors, e.g. -2419.38(10) means -2419.38 ± 0.10.

The geometry of the molecules that were used in the LEQUOR, and size and shape programs are as presented in Table IV.2. The input coordinates of the atoms of iodobenzene, chlorobenzene, 1,2-dichloro-benzene, 1,3-dichlorobenzene, 1,2-dicyanobenzene, 1,3-dinitrobenzene and 2,6-di-fluoropyridine were calculated using data from the literature. For iodobenzene, the calculations of the atomic positions were based on the assumption that it is a regular hexagon. Calculations of 1,3-di-nitrobenzene involved using a geometry from electron diffraction studies, and for 1,2-dicyanobenzene using that from a liquid crystal NMR study. The atomic coordinates of 2,6-difluoropyridine, chlorobenzene, 1,2-dichlorobenzene, and 1,3-dichlorobenzene were calculated from micro-wave data.

Results of the analysis from the program SHAPE: the set of experi-mental order parameters S_{xx}, S_{yy} and S_{zz}, and the relative geometry as determined from the dipolar couplings of the solutes dissolved in 55 wt% 1132 are as listed in Tables IV.3 and IV.2 respectively. For acetone, a modified version of SHAPE was used to obtain the order parameters. The modified program takes into account the rotation of the methyl groups.

The predicted order parameters were obtained by integrating equa-tions [17] using the size and shape program with the geometry of the molecules (Table IV.2) as input. The values of S calculated as given in Table IV.3 are accurate to four figures. The value of k = 5.2 dyne/cm has been determined by a least squares fit of calculated and experi-mental S.

The relative internuclear distances of a molecule are determined using equation [6]. From Table IV.2 it is noted that the output coordi-

nates that were varied agree to within ± 0.03 Å with the values from the literature except for TTF and 1,3-dinitrobenzene. The discrepancies observed in these two molecules may be due to one of the dipolar couplings being not accurately determined and of a small magnitude. The relative internuclear distance ratios calculated using this coupling are then imprecise.
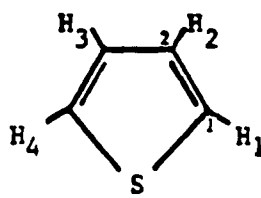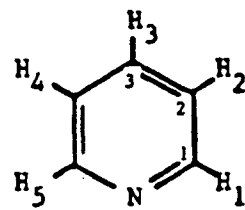
Table IV.2:   The geometry of the molecules (i) literature[a]
Y   (ii) experimental[b] - presented in brackets.
The axis system for all the molecules is as shown here.
The z-axis points out from the page.
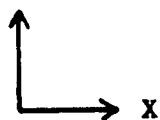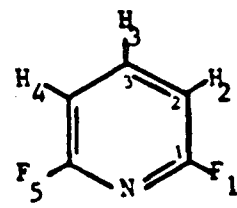
Molecules	Atom[c]	X	Coordinates (Å) Y	Z	Radius[d]	Ref.
1 TTF	C_1	3.1930	-0.6572	-0.3743	1.75	31
	C_3	0.6745	0	0	1.75	
	S_1	1.6250	1.4777	0	1.75	
	H_1	-3.9975	1.2151	0.6640	1.20	
		(-3.811(7))	(1.2151)	(0.6640)		
2 Acetone	C_1	0	0	0	1.69	45
	C_2	-0.7700	1.3337	0	1.70	
	O	1.2220	0	0	1.50	
	H_1	-1.3968	1.3919	0.8898	1.20	
	H_2	-0.0621	2.1625	0	1.20	
	H_3	-1.3968	1.3919	-0.8898	1.20	
3 Furan	C_1	1.0920	0	0	1.77	46
	C_2	0.7160	1.3080	0	1.77	
	O	0	-0.8140	0	1.50	
	H_1	2.0466	-0.8132	0	1.00	
		(2.0466)	(-0.8132)	(0)		
	H_2	1.3777	1.8376	0	1.00	
		(1.3743(1))	(1.8119(17))	(0)		
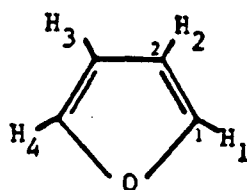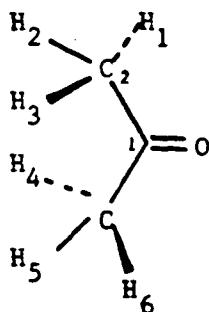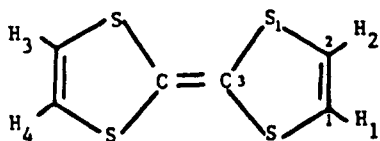
4 Thiophene

C_1	1.2360	0.0463	0	1.77	47
C_2	0.7116	1.3121	0	1.77	
S	0	-1.1426	0	1.75	
H_1	2.2692	-0.2550	0	1.00	
	(2.2692)	(-0.2550)	(0)		
H_2	1.3201	2.2050	0	1.00	
	(1.3226(6))	(2.2341(4))	(0)		

5 Pyridine

C_1	1.1416	-0.6929	0	1.77	48
C_2	1.1974	0.7005	0	1.77	
C_3	0	1.4151	0	1.77	
N	0	-1.3949	0	1.55	
H_1	2.0557	-1.2761	0	1.01	
	(2.054(3))	(-1.245(9))	(0)		
H_2	2.1526	1.2055	0	1.01	
	(2.1526)	(1.2055)	(0)		
H_3	0	2.4924	0	1.01	
	(0)	(2.4924)	(0)		

6 2,6-Difluoro-pyridine

C_1	1.1110	0.7080	0	1.77	calculated from 49
C_2	1.2070	2.0810	0	1.77	
C_3	0	2.7800	0	1.77	
N	0	0	0	1.56	
F_1	2.2430	-0.0220	0	1.47	
	(2.2430)	(-0.220)	(0)		

H$_2$	2.1710	2.5680	0	1.01	
	(2.1779(10))	(2.5629(5))	(0)		
H$_3$	0	3.8620	0	1.01	
	(0)	(3.8620)	(0)		

7 Fluorobenzene	C$_1$	0	-0.8490	0	1.77	50
	C$_2$	1.2170	-0.1930	0	1.77	
	C$_3$	1.2080	1.2020	0	1.77	
	C$_4$	0	1.9030	0	1.77	
	F	0	-2.2030	0	1.47	
		(0)	(-2.2030)	(0)		
	H$_2$	2.1370	-0.7610)	0	1.01	
		(2.1501(6))	(-0.7616(4))	(0)		
	H$_3$	2.1460	1.7430	0	1.01	
		(2.1644(6))	(1.7437(4))	(0)		
	H$_4$	0	2.9830	0	1.01	
		(0)	(2.9830)	(0)		
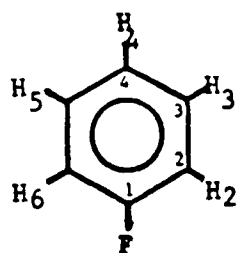
8 Chlorobenzene	C$_1$	0	1.4002	0	1.77	calculated from 51
	C$_2$	1.2126	-0.7001	0	1.77	
	Cl	0	-3.1112	0	1.77	
	H$_1$	2.1400	-0.2830	0	1.01	
		(2.109(2))	(-0.2823(12))	(0)		
	H$_2$	2.1454	2.1817	0	1.01	
		(2.1454)	(2.1817)	(0)		
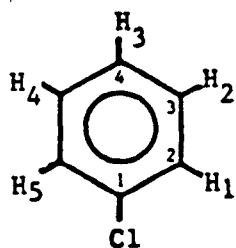
H$_3$	0	3.4260	0	1.01	
	(0)	(3.4260)	(0)		

9 Iodobenzene	C$_1$	0	1.3970	0	1.77	assumed regular hexagon 52
	C$_2$	1.2098	-0.6985	0	1.77	
	I	0	-3.4770	0	2.06	
	H$_1$	2.1486	1.2405	0	1.01	
		(2.1486)	(1.2405)	(0)		
	H$_2$	2.1486	-1.2405	0	1.01	
		(2.170(2))	(-1.237(3))	(0)		
	H$_3$	0	-2.4810	0	1.01	
		(0)	(-2.4810)	(0)		
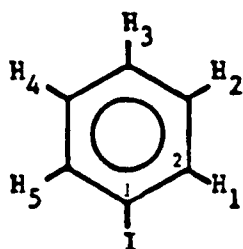
10 1,2-Dichloro-benzene	C$_1$	0.6985	-1.2098	0	1.77	calculated from 53
	C$_2$	1.3970	0	0	1.77	
	Cl$_1$	1.5338	-2.7168	0	1.77	
	H$_1$	2.4810	0	0	1.01	
		(2.4520(17))	(0)	(0)		
	H$_2$	1.2405	2.1846	0	1.01	
		(1.2405)	(2.1846)	(0)		
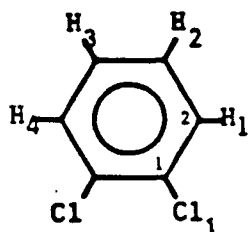
11 1,2-Dicyano-benzene	C$_1$	1.4420	-3.6530	0	1.78	calculated from 40
	C$_2$	0.7035	-2.4191	0	1.77	
	C$_3$	1.4165	-1.2043	0	1.77	
	C$_4$	0.6955	0	0	1.77	
	N$_1$	2.0318	-4.5933	0	1.70	
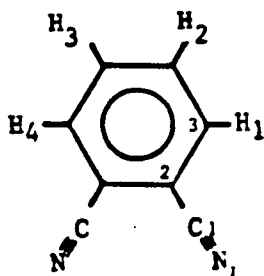
			x	y	z	r	
		H_1	2.4803	-1.2043	0	1.01	
			(2.45(14))	(-1.24(9))	(0)		
		H_2	1.2388	0.9334	0	1.01	
			(1.2388)	(0.9334)	(0)		
12	1,3-Dichloro-benzene	C_1	0	1.3960	0	1.77	calculated from 54
		C_2	-1.2090	-0.6980	0	1.77	
		Cl_1	2.6906	1.5638	0	1.77	
		H_1	0	2.4800	0	1.01	
			(0)	(2.4800)	(0)		
		H_2	-2.1480	-1.2400	0	1.01	
			(-2.1470(17))	(-1.2356(6))	(0)		
		H_3	0	2.4800	0	1.01	
			(0)	(2.4800)	(0)		
13	1,3-Dinitro-benzene	C_1	0	0.699	0	1.77	calculated from 55,56
		C_2	-1.870	0	0	1.77	
		C_3	-1.307	-1.373	0	1.77	
		C_4	0	-2.152	0	1.77	
		N_1	2.428	0.763	0	1.55	
		O_1	3.435	0.207	0.425	1.40	
		O_2	2.386	1.912	-0.425	1.40	
		H_1	0	1.789	0	1.01	
			(0)	(1.789)	(0)		
		H_2	-2.2920	-1.839	0	1.01	
			(-2.170(9))	(-1.996(3))	(0)		
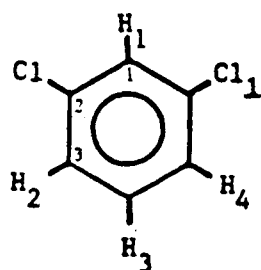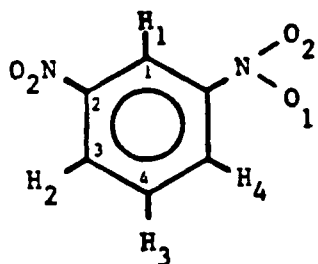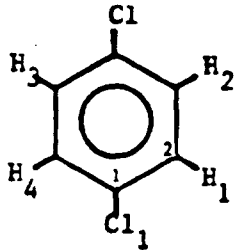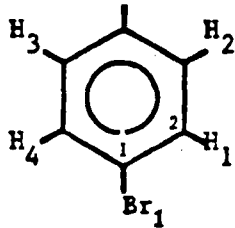
H_3	0	-3.242	0	1.01	
	(0)	(-3.242)			
14 1,4-Dichloro-benzene					
C_1	0	-1.375	0	1.77	43
C_2	1.213	-0.697	0	1.77	
Cl_1	0	-3.105	0	1.77	
H_1	2.162	1.253	0	1.01	
	(2.162)	(1.255(1))	(0)		
15 1,4-Dibromo-benzene					
C_1	0	-1.375	0	1.77	44
C_2	1.213	-0.697	0	1.77	
Br_1	0	-3.215	0	1.92	
H_1	2.170	-1.252	0	1.01	
	(2.165(1))	(-1.252)	(0)		

a These coordinates were used as input into the programs LEQUOR, and size and shape.

b These proton coordinates were determined from dipolar couplings of the solutes dissolved in 55 wt % 1132. The numbers are presented in brackets, e.g. (-3.8106(12)) where (12) is the uncertainty in the last two decimal places. The coordinates with errors were varied during the calculation using SHAPE. The coordinates without errors were fixed as scaling factors during calculation.

c Coordinates not shown are fixed by symmetry.

d The values of radii were taken from Ref. 57.

Table IV.3:   Experimental and calculated order parameters of solutes
              dissolved in the nematic liquid crystal of 55 wt% 1132
              mixture at 301.4 K

	Molecule[a]		Order Parameter	
			Experimental[b]	Calculated[c]
1	TTF	S_{xx}	0.3320 (17)	0.3859
		S_{yy}	-0.081 (3)	-0.1402
		S_{zz}	-0.2514 (17)	-0.2457
2	Acetone	S_{xx}	0.0090 (1)	-0.0031
		S_{yy}	0.0711 (2)	0.0712
		S_{zz}	-0.0720 (1)	-0.0681
3	Furan	S_{xx}	0.0907 (1)	0.0602
		S_{yy}	-0.0458 (2)	0.0247
		S_{zz}	-0.1365 (1)	-0.0849
4	Thiophene	S_{xx}	0.0586 (1)	0.0519
		S_{yy}	0.0905 (5)	0.0428
		S_{zz}	-0.1490 (4)	-0.0947
5	Pyridine	S_{xx}	0.1093 (2)	0.0690
		S_{yy}	0.0452 (6)	0.0394
		S_{zz}	-0.1545 (4)	-0.1084

6	2,6-Difluoro-pyridine	S_{xx}	0.1529 (2)	0.1165
		S_{yy}	0.0379 (4)	0.0266
		S_{zz}	-0.1908 (2)	-0.1431
7	Fluorobenzene	S_{xx}	0.0507 (1)	0.0236
		S_{yy}	0.1399 (2)	0.1081
		S_{zz}	-0.1906 (1)	-0.1317
8	Chlorobenzene	S_{xx}	0.0070 (1)	-0.0092
		S_{yy}	0.1967 (3)	0.1520
		S_{zz}	-0.2037 (2)	-0.1428
9	Iodobenzene	S_{xx}	-0.0243 (5)	-0.0547
		S_{yy}	0.2389 (11)	0.2196
		S_{zz}	-0.2146 (6)	-0.1649
10	1,2-Dichlorobenzene	S_{xx}	0.0647 (1)	0.0254
		S_{yy}	0.1601 (2)	0.1419
		S_{zz}	-0.2248 (3)	-0.1673
11	1,2-Dicyanobenzene	S_{xx}	0.063 (11)	0.0277
		S_{yy}	0.184 (24)	0.1729
		S_{zz}	-0.247 (13)	-0.2006

12	1,3-Dichlorobenzene	S_{xx}	0.1958 (4)	0.1916
		S_{yy}	0.0285 (7)	-0.0134
		S_{zz}	-0.2243 (3)	-0.1782
13	1,3-Dinitrobenzene	S_{xx}	0.242 (3)	0.2092
		S_{yy}	0.040 (4)	-0.0092
		S_{zz}	-0.282 (1)	-0.2000
14	1,4-Dichlorobenzene	S_{xx}	-0.0721 (1)	-0.0976
		S_{yy}	0.3188 (5)	0.2879
		S_{zz}	-0.2467 (4)	-0.1903
15	1,4-Dibromobenzene	S_{xx}	-0.1021 (1)	-0.1331
		S_{yy}	0.3567 (2)	0.3395
		S_{zz}	-0.2546 (1)	-0.2064

[a] The molecular axis system of the molecules is as in Table IV.2

[b] Order parameters obtained from the experimental dipolar coupling constants. The bracketed numbers are errors.

[c] Order parameters calculated using the size and shape program with coordinates in Table IV.2 as input. These values have been fitted by the least squares method to obtain optimal agreement with experimental values.

IV.2 Furan and Thiophene

The proton spectra of furan and thiophene obtained in:

(i) 55 wt% 1132 in the temperature range 304-325 K (dial T) and

(ii) the component liquid crystals: 1132 and EBBA at 301.4 K

were similarly analyzed using LEQUOR and SHAPE. The geometries used were from Table IV.2 and the indirect couplings from Ref. 33 and 34. The experimental spectral parameters are listed in Tables IV.4 and IV.5 and the orientation parameters in Tables IV.6 and IV.7. In the temperature study, it was noted that the magnitude of all the order parameters decrease steadily with increase in temperature.

Table IV.4: Experimental dipolar couplings[a] (Hz), the chemical shift differences (Hz), and the rms errors[b] (Hz) obtained from LEQUOR for furan and thiophene dissolved in the nematic liquid crystal 55 wt% 1132 at various temperatures.

Temperature (K) (dial T)	Parameter	Furan[c]	Thiophene[c]
306	D_{12}	-289.05 (6)[d]	-538.84 (3)
	D_{13}	-108.43 (7)	- 97.03 (4)
	D_{14}	-154.69 (6)	- 73.47 (6)
	D_{23}	-511.23 (7)	-371.27 (6)
	$\nu_2 - \nu_1$	372.68 (12)	85.31 (14)
	rms	0.20	0.14
308	D_{12}	-285.61 (15)	-528.23 (3)
	D_{13}	-106.16 (16)	- 94.91 (3)
	D_{14}	-151.07 (15)	- 71.77 (5)
	D_{23}	-499.01 (18)	-362.66 (5)
	$\nu_2 - \nu_1$	373.5 (3)	85.43 (12)
	rms	0.45	0.12
310	D_{12}	-281.87 (5)	-517.34 (2)
	D_{13}	-103.87 (6)	- 92.77 (2)
	D_{14}	-147.34 (6)	- 70.00 (4)
	D_{23}	-486.76 (7)	-354.08 (4)
	$\nu_2 - \nu_1$	374.79 (12)	85.42 (10)
	rms	0.17	0.10

312	D_{12}	-277.88 (3)	-505.86 (3)
	D_{13}	-101.53 (4)	- 90.56 (3)
	D_{14}	-143.58 (4)	- 68.24 (5)
	D_{23}	-474.39 (4)	-344.91 (5)
	$\nu_2 - \nu_1$	376.00 (7)	85.63 (13)
	rms	0.19	0.12
314	D_{12}	-273.46 (4)	-493.96 (3)
	D_{13}	- 99.11 (5)	- 88.22 (4)
	D_{14}	-139.64 (5)	- 66.42 (7)
	D_{23}	-461.20 (6)	-335.75 (7)
	$\nu_2 - \nu_1$	377.35 (10)	85.68 (15)
	rms	0.12	0.15
320	D_{12}	-259.88 (12)	-452.47 (5)
	D_{13}	- 91.82 (13)	- 80.33 (6)
	D_{14}	-128.62 (13)	- 60.29 (11)
	D_{23}	-425.54 (17)	-304.61 (11)
	$\nu_2 - \nu_1$	380.4 (3)	85.9 (3)
	rms	0.34	0.24
325	D_{12}	-243.48 (14)	-413.8 (2)
	D_{13}	- 84.52 (16)	- 73.4 (3)
	D_{14}	-117.17 (16)	- 54.3 (5)
	D_{23}	-387.10 (2)	-276.9 (5)

$\nu_2 - \nu_1$	384.0	(3)	86	(1)
rms	0.47		1.10	

---

a   The numbering of furan and thiophene is as in Table IV.2.

b   Rms error of the fit of the experimental to the calculated spectra by the program LEQUOR.

c   The indirect couplings are as in Table IV.1.

d   Numbers in brackets refer to errors.

Table IV.5[a]: Experimental dipolar couplings (Hz), the chemical shift differences (Hz), and the rms errors (Hz) obtained from LEQUOR for furan and thiophene dissolved in the nematic liquid crystals 1132 and EBBA at 301.4 K.

Liquid Crystal		Spectral Parameters	
		Furan	Thiophene
1132	D_{12}	-253.42 (18)[b]	-695.95 (4)
	D_{13}	-181.06 (19)	-160.76 (4)
	D_{14}	-302.39 (9)	-143.64 (6)
	D_{23}	-996.93 (10)	-723.01 (6)
	$\nu_2 - \nu_1$	332.77 (2)	49.46 (15)
	rms	0.34	0.16
EBBA	D_{12}	-349.86 (3)	-460.82 (11)
	D_{13}	- 36.12 (4)	- 29.52 (13)
	D_{14}	- 2.93 (4)	10.50 (4)
	D_{23}	- 13.31 (4)	50.8 (4)
	$\nu_2 - \nu_1$	416.79 (10)	143.1 (2)
	rms	0.13	0.48

a   Indirect couplings used are as in Table IV.1.

b   Numbers in brackets denote errors.

Table IV.6[a]: Experimental order parameters of furan and thiophene
dissolved in the liquid crystal 55 wt% 1132 at various
temperatures.

Temperature (K) (dial T)		Order Parameter[b]	
		Furan	Thiophene
304	S_{xx}	0.0907 (1)	0.0586 (1)
	S_{yy}	0.0457 (2)	0.0905 (5)
	S_{zz}	-0.1365 (1)	-0.1490 (4)
306	S_{xx}	0.0884 (1)	0.0572 (1)
	S_{yy}	0.0452 (3)	0.0887 (3)
	S_{zz}	-0.1335 (2)	-0.1459 (2)
308	S_{xx}	0.0863 (1)	0.0559 (1)
	S_{yy}	0.0448 (5)	0.0868 (3)
	S_{zz}	-0.1311 (4)	-0.1427 (2)
310	S_{xx}	0.0841 (1)	0.0545 (1)
	S_{yy}	0.0443 (3)	0.0850 (3)
	S_{zz}	-0.1285 (2)	-0.1395 (2)
312	S_{xx}	0.0820 (1)	0.0531 (1)
	S_{yy}	0.0437 (2)	0.0832 (3)
	S_{zz}	-0.1258 (1)	-0.1363 (2)

314	S_{xx}	0.0798 (1)	0.0517 (1)
	S_{yy}	0.0430 (2)	0.0809 (3)
	S_{zz}	-0.1227 (1)	-0.1326 (2)
320	S_{xx}	0.0735 (1)	0.0469 (1)
	S_{yy}	0.0418 (5)	0.0737 (5)
	S_{zz}	-0.1152 (4)	-0.1206 (4)
325	S_{xx}	0.0669 (1)	0.0423 (4)
	S_{yy}	0.0389 (7)	0.0690 (21)
	S_{zz}	-0.1055 (6)	-0.1113 (17)

---

[a] The molecular axis system of furan and thiophene is as in Table IV.2.

[b] The numbers in brackets denote errors.

Table IV.7: Experimental order parameters of furan and thiophene in 1132 and EBBA at 301.4 K

| Liquid Crystal | | Order Parameters [a] | |
		Furan	Thiophene
1132	S_{xx}	0.1727 (1)	0.1118 (1)
	S_{yy}	0.0336 (3)	0.0871 (5)
	S_{zz}	-0.2063 (2)	-0.1990 (4)
EBBA	S_{xx}	0.0017 (1)	-0.0082 (3)
	S_{yy}	0.0548 (4)	0.0819 (13)
	S_{zz}	-0.0565 (3)	-0.0737 (10)

[a] The numbers in brackets denote errors.

CHAPTER V

DISCUSSION

V. DISCUSSION

The   component, S_{pq},   of the order tensor of a molecule is given by the expression:

$$S_{pq} = (1/2) <3 \cos\theta_p \cos\theta_q - \delta_{pq}> \qquad [8]$$

$$p,q = x, y, z$$

Equation [8] defines the range of the order parameter to be $-0.5 \leq S \leq 1$ for $p = q$.   For example if $S_{zz} = 1$, the molecule fixed z-axis is on average oriented parallel to the applied magnetic field; and if $S_{zz} = -0.5$, perpendicular to it.   For $S_{zz} = 0$, there are two possible contributing factors:

(i) the average orientation of the molecular z-axis is at 54.74° or

(ii) all orientations of the z-axis are equally probable.

The orientation of a molecule in a liquid crystalline system is dependent on the type of interactions between the solvent and solute molecules.   In the recent study by van der Est et al.[22] the size and shape, and the efg-quadrupole moment interactions were found to play important roles in the orientation of a series of solutes. The size and shape mechanism is further investigated in this work.

The liquid crystal solvent used for the study of this mechanism is the 55 wt% 1132 mixture. In this liquid crystal, D_2 experiences a zero electric field gradient, and it is assumed that other solutes experience

the same zero efg. All the samples used were made by dissolving the minimum amount of solute (1 mole percent) in the liquid crystal. This concentration approximates infinite dilution where there is least disruption in the ordering of the liquid crystal molecules.

V.1 Orientation of Solutes in 55 wt% 1132 - Qualitative Survey

From the results of the variety of solutes dissolved in 55 wt% 1132 (Table IV.3), it is noted that generally the axes of longest molecular dimensions have the most positive S-values. This agrees with one's intuition that solutes should tend to orient with their longest molecular dimension along the director of the liquid crystal, where least disruption of the liquid crystal molecules is caused. This is clearly seen in the molecule TTF. On average, it orients such that the greatest length of the molecule is along the director axis.

An examination of the monosubstituted benzenes showed that the size of the solutes is important in determining their orientation. The order parameters of fluorobenzene: $S_{xx} = 0.0507$, $S_{yy} = 0.1399$ and $S_{zz} = -0.1906$ indicate that the C_2 axis and the plane of the ring of this solute is aligned preferentially along the nematic axis. This is even more pronounced in the case of chlorobenzene and iodobenzene. In this series of three molecules, as the substituent halogen increases in size, S_{xx} progressively decreases and S_{yy} increases. This indicates that as the substituent halogen atom becomes larger, the C-X direction (X = halogen) i.e. the y axis, becomes more oriented along the director axis.

On comparing results for 1,2-dichlorobenzene and 1,2-dicyanobenzene it is noted that the symmetry axis of the cyano-substituted ring is more aligned along the nematic axis than that of dichlorobenzene. This is expected because the cyano-group is bigger and longer along the y-direction of the molecule-fixed axis than the chlorine atoms. This trend is also observed in the 1,4-disubstituted benzenes. The more bulky dibromobenzene is oriented with its symmetry axis preferentially along the nematic axis as compared to 1,4-dichlorobenzene. It is also interesting to note the results obtained for the following series of compounds: chloro-, 1,2-dichloro-, 1,3-dichloro- and 1,4-dichloro-benzene. The orientation of the ring changes with the position of substitution of chlorine atoms. In each case, the solute is aligned such that the longest molecular dimension is along the director axis.

For molecules which have similar length and breadth dimensions, it is not obvious as to which orientation is favored. This is seen in the case of acetone. The order parameters are all quite small indicating that the orientation is almost equally probable in all directions. This brief survey of the results obtained for C_{2v}^{*} molecules shows that generally their molecular dimensions are important in determining their orientation. Thus in trying to understand the mechanism responsible, the size and shape model proposed by van der Est[22] is used to determine orientational order in these molecules.

V.2   The Size and Shape Model

V.2.1   Prediction of Orientation of Solutes

The size and shape model takes only the short range repulsive forces acting between solute and liquid crystal molecules to be responsible for orientation. The mean field approach is used where the liquid crystal molecules are replaced by an anisotropic continuum; they are modelled as an elastic tube. The solute molecules, assumed rigid, fit into and stretch this tube. The mean potential energy of the system arises from this stretching of the elastic walls of the tube by the solute molecules. The two interacting surfaces i.e. that of the solutes and the tube, are assumed to be hard surfaces. These short range interactions are dependent on the size and shape of the solutes (see Theory). This model ignores specific interactions, for example H-bonding, and will break down in the presence of such interactions.

The model is used to predict the orientational parameters of all the solutes in this 55 wt% 1132 system (see Section III.2). The calculated parameters: S_{xx}, S_{yy} and S_{zz} are plotted against the experimental results in Figs. V.1, V.2, and V.3 respectively. The van der Waals radii were taken from Ref. 57. The adjustable parameter, the force constant, k, was obtained by a least squares fit procedure using two independent parameters S_{xx}-S_{yy} and S_{zz}, of all the solutes to obtain optimal agreement between theoretical and experimental results. The value of k was found to be 5.2 dyne/cm. As can be seen from the plots, the correlation is good. In Figs. V.1 and V.2, it is noted that most of

Fig. V.1   Size and shape model: calculated versus experimental order
parameters S_{xx} of solutes in 55 wt% 1132.   The labelling of
the points refers to molecules indicated in Table IV.2
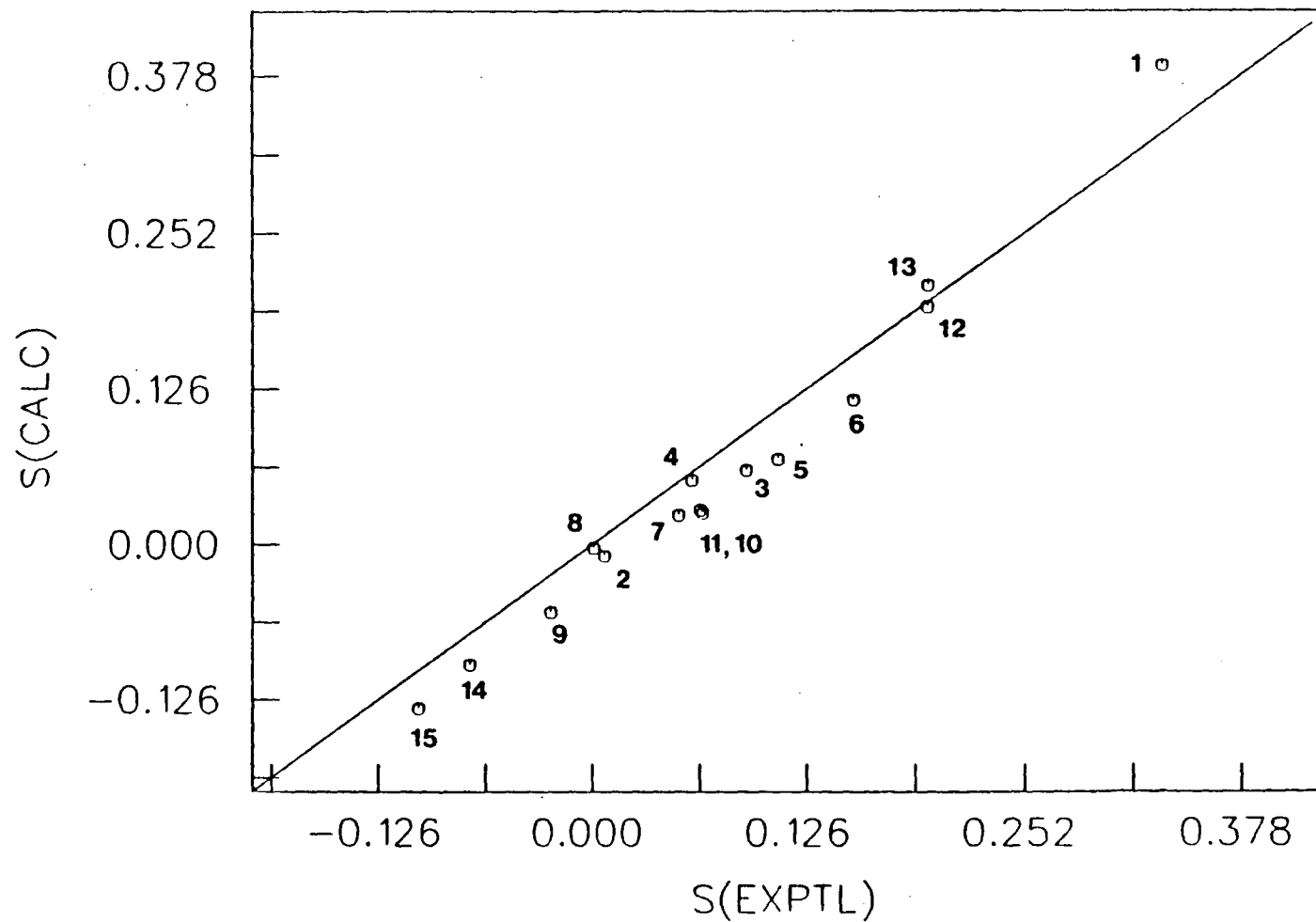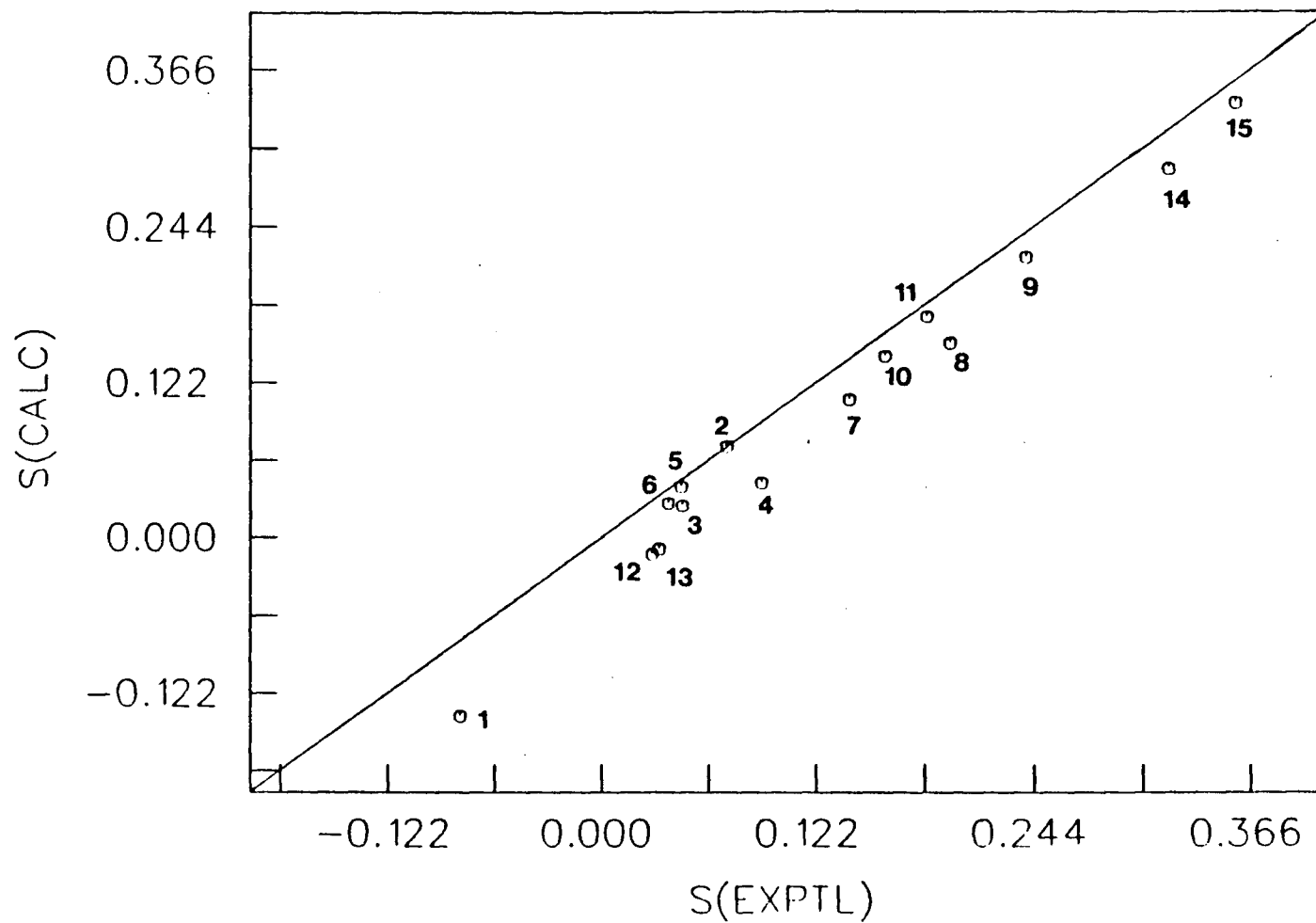
Fig. V.2   Size and shape model: calculated versus experimental order parameters S_{yy} of solutes in 55 wt% 1132. The labelling of points refers to molecules listed in Table IV.2

the points lie below the unit slope line i.e. the predicted values for S_{xx} and S_{yy} are generally smaller than experimental values. Since the order matrix is traceless, the S_{zz} calculated are then larger than experimental results (Fig. V.3). The observed deviations can be explained by factors discussed in the next section.

Fig. V.4 shows a plot of the asymmetry parameter η, calculated versus experimental. This parameter is defined as:

$$\eta = \frac{S_{xx} - S_{yy}}{S_{zz}} \qquad [18]$$

The two independent parameters S_{xx}-S_{yy} and S_{zz} describe the orientation of the same solute, and are dependent on the environment in the same way. η is independent of the force constant (for small k) indicating that this ratio is to a good approximation independent of the environment. This allows one to determine how well the relationship between order parameters of individual solutes is predicted. Consequently, it is a better indication of how good the correlation is between calculated and experimental results for each solute. As can be seen from the plot of η in Fig. V.4, although there are some deviations, the correlation is remarkably good indicating that the orientation is well predicted for each solute.

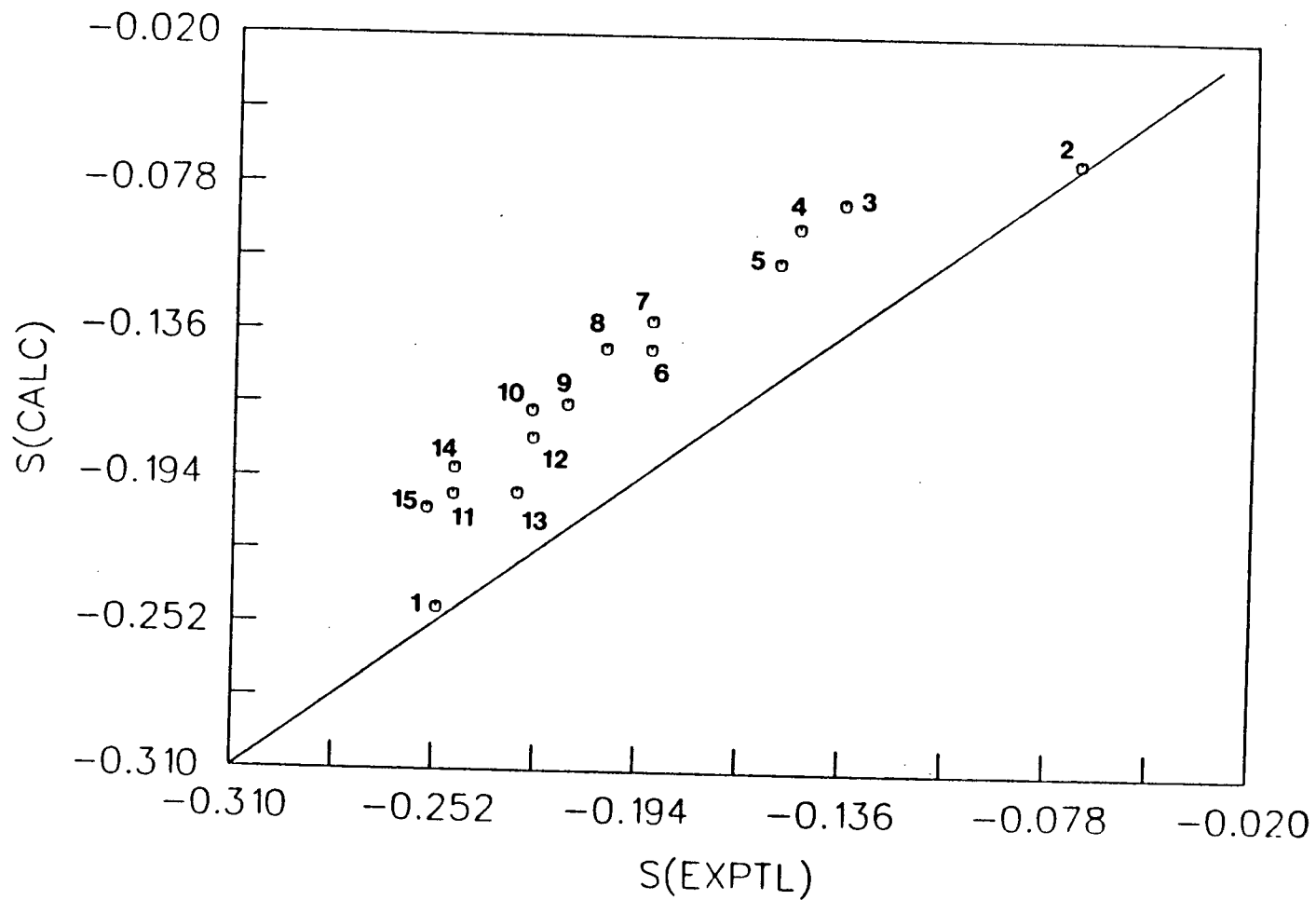Fig. V.3   Size and shape model: calculated versus experimental order parameters S_{zz} of solutes in 55 wt% 1132.   The labelling of points refers to molecules listed in Table IV.2
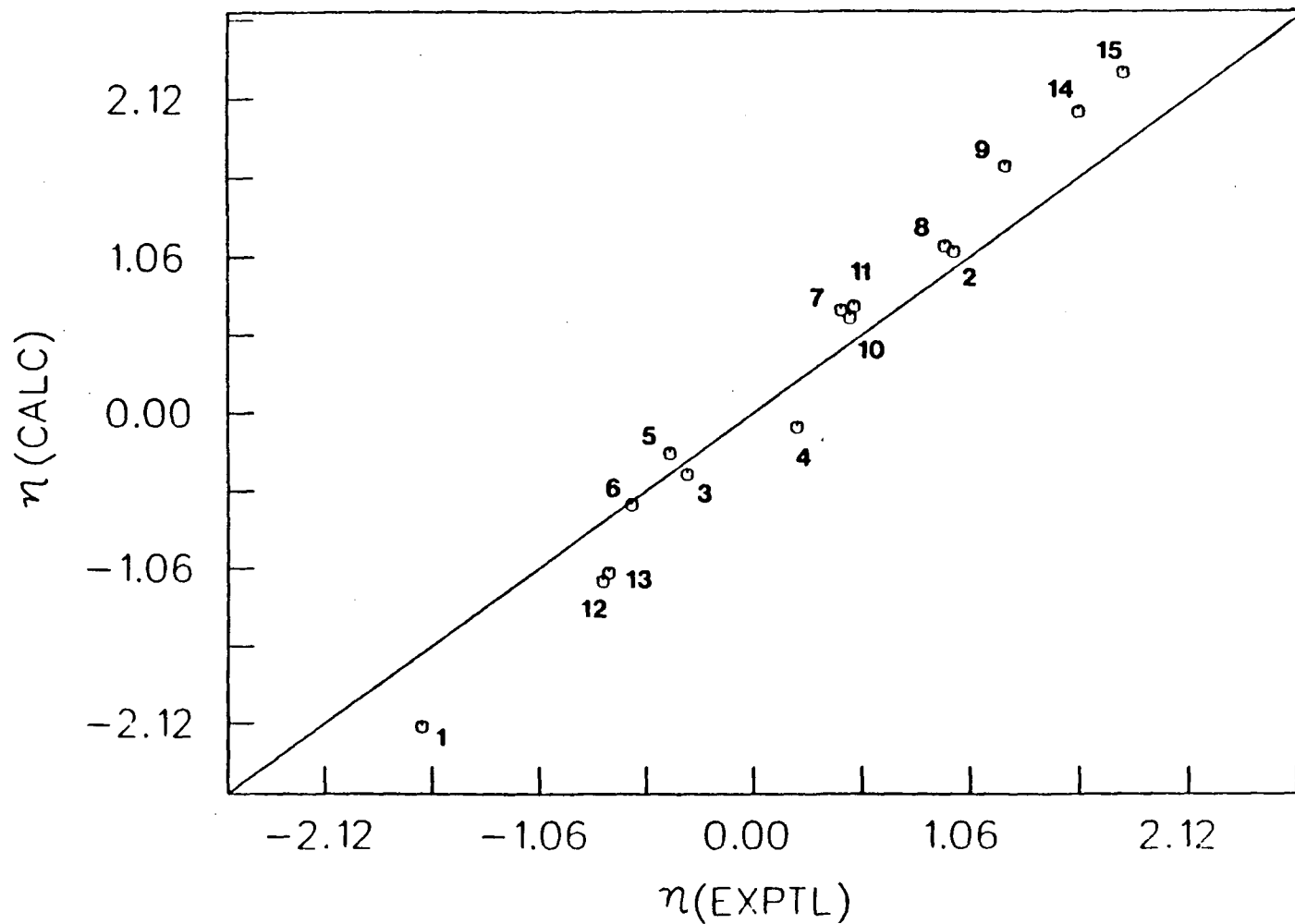
Fig. V.4   Size and shape model: calculated versus experimental

parameters $\eta = \dfrac{S_{xx} - S_{yy}}{S_{zz}}$ of solutes in 55 wt% 1132.   The

numbering of points are the molecules listed in Table IV.2

V.2.2   Factors Causing Deviations in Predicted Orientations

The slight deviations from the experimental parameters of the solutes as observed in Figs. V.1, V.2, V.3, and V.4 can be explained in terms of the assumptions made in studying this system. The size and shape picture that was used is not an exact and accurate description of the liquid crystalline system. As mentioned, the mean field approach is taken where the individual liquid crystal molecules are replaced by a continuum. All the solutes are assumed to experience a mean environment. This is not so in the actual system where the liquid crystal molecules are flexible and exist in many different conformations. Therefore an exact description of the system would involve all the conformations of the liquid crystal molecules. Since these molecules are replaced by an average environment in the size and shape model, the predicted order parameters will differ from the experimental values. However, as the deviation is not of a large magnitude, the mean field description of the system is adequate. In fact the correlation is surprisingly much better than expected for this simplistic picture.

In the model used, it was also assumed that all the solute molecules experience the same mean environment. All the molecules are assumed to experience no field gradient based on the fact that D_2 experiences a zero efg. The EBBA molecules are long and consist of two benzene rings and an alkyl chain. It is likely that the electric field gradient near the rings will differ from that which is close to the alkyl chains. D_2, being a small molecule can occupy certain 'sites' where it sees a zero efg. Other large solute molecules may not occupy

the same 'sites'. This has been shown by Buckingham et al.[58] in the case of tetramethylsilane (TMS), CH_4, CF_4 and SF_6. These molecules occupy different sites as indicated by differences in local solvent anisotropy effects (on the chemical shielding). In this study, the larger solute molecules may not occupy the same 'sites'. Consequently they will experience different environments e.g. the presence of some efg due to their proximity to different parts of the liquid crystal molecules. Thus some efg-molecular quadrupole moment interactions may be present and this would contribute towards the orientation of the molecules. Consequently deviations from the predicted parameters will then be seen.

Different mean environments may also arise from slight concentration and temperature variations in different samples. The order parameter S is to a good approximation proportional to the interaction energy U, which is in turn dependent on the product of two factors as given below:

$$S \approx \frac{KU}{k_B T} \approx C \frac{GB}{k_B T} \tag{[19]}$$

where

    K and C are constants

    G is some property of the liquid crystal

    B is some property of the solutes

This equation applies only when $\frac{KU}{k_B T} \ll 1$.

G is a function of the order parameter of the liquid crystal molecules. Altering the concentration of the solute molecules will affect the ordering of the liquid crystals. The value of G is then changed and this will, in turn, vary the order parameter S of the solutes. This is also intuitively obvious in that increasing the number of solute molecules will cause a disruption in the ordering of the liquid crystal molecules which then allows more orientational freedom in the solutes. In the model, S was calculated assuming infinite dilution of the solutes where there is no disruption in the properties of the liquid crystals. The other factor affecting S is the temperature of the system. The higher the temperature the lower the order parameter. The presence of these two factors thus affects the value of S of the different solutes studied.

Another possible factor is that the model used considered only short range hard body interactions to be responsible for orientation in the molecules. This does not, however, mean that there are no other types of interactions present. Short range attractive forces between molecules were ignored and so were long range interactions. All these if present could cause some deviations between experimental and theoretical results.

Therefore, by considering some of the assumptions of the model, the small deviations in the calculated parameters can be accounted for. In general, it has been shown that the orientation of the series of C_{2v}^{*} molecules in 55 wt% 1132 can be predicted well with the size and shape model. This picture is successful in modelling the short range hard body interaction, and thus the mean field approach, although simple, is

an adequate description. The results of this study give strong evidence that the size and shape of solutes is important in determining their orientation. Although other mechanisms related to the dimensions of the solutes cannot be completely ruled out, it can be concluded that short range repulsive interactions must play a very important role.

V.2.3 Effects of Temperature and Concentration Variations

An attempt was made to determine if the correlation between experimental and predicted parameters could be improved by removing concentration and temperature variations among samples. In this study the liquid crystal EBBA was deuterated at two ring positions. (A set of results were also obtained for the series of solutes in a mixture of 55 wt% 1132 where the EBBA molecules were not deuterated. The results are presented in the Appendix).
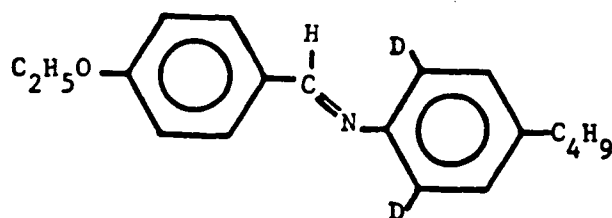
The deuteron spectrum of this compound is as shown in Fig. IV.3. The two C-D directions of the EBBA in the 55 wt% mixture give two doublets with quadrupolar splittings of 19 and 16 kHz in the spectrum. The splittings provide a measure of the ordering of the liquid crystal molecules. Therefore, any differences in the liquid crystal environment

will affect the splittings. The more disorder there is, the smaller will be the splittings. Thus, any effects due to varying concentration of the solutes and temperature which disrupt the liquid crystal molecules should show up in the splittings in the deuteron spectrum. For each sample, a deuteron spectrum was collected and the quadrupolar splittings measured. The experimental order parameters were scaled as follows:

$$S_{scaled} = \frac{\Delta\nu_{D_2}}{\Delta\nu_{solute}} \times S_{exptl} \qquad [20]$$

where

$\Delta\nu_{D_2}$ is the quadrupolar splittings of EBBA in the sample of D_2 in 55 wt% 1132 mixture

$\Delta\nu_{solute}$ is the quadrupolar splittings of EBBA in the individual solute sample.

The standard chosen for scaling was the splitting from the D_2 sample because this was used to determine the efg in the mixture. The two sets of experimental order parameters, scaled and unscaled, are compared with the theoretical values in the following two figures. Fig. V.5 is the plot of all the S (unscaled) versus calculated values. The k value obtained from the least squares fit of these results is 5.2 dyne/cm, and the correlation coefficient is 0.980. The plot of S (scaled) versus theoretical values is as shown in Fig. V.6. The k value here is 5.3 dyne/cm, and the correlation coefficient is 0.979. Unscaled order parameters and k values were reported in section IV and throughout the
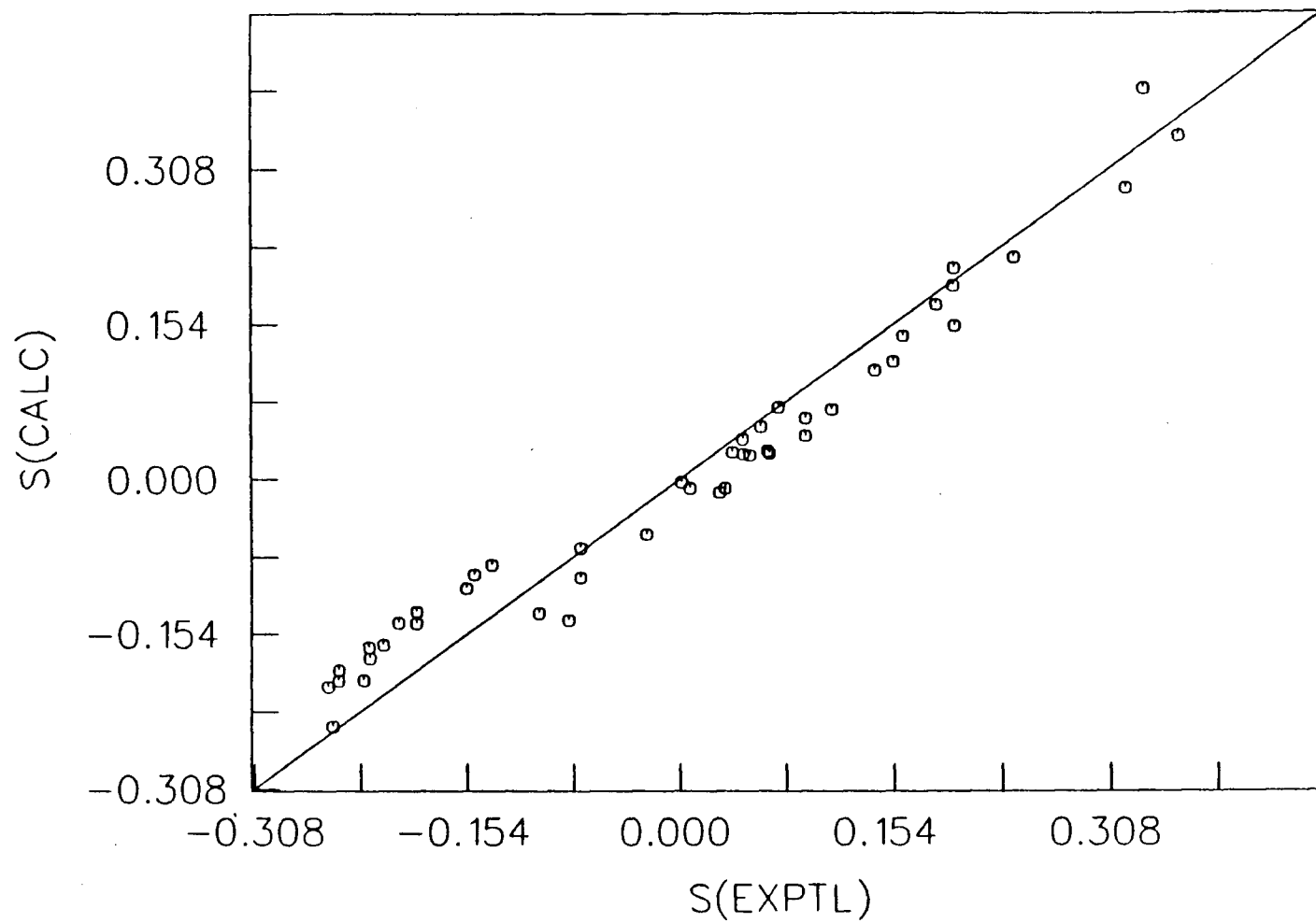
Fig. V.5   Theoretical versus unscaled experimental order parameters:
S_{xx}, S_{yy} and S_{zz} of solutes in 55 wt% 1132.   The k value from
the least squares fit of this data is 5.2 dyne/cm.   Correla-
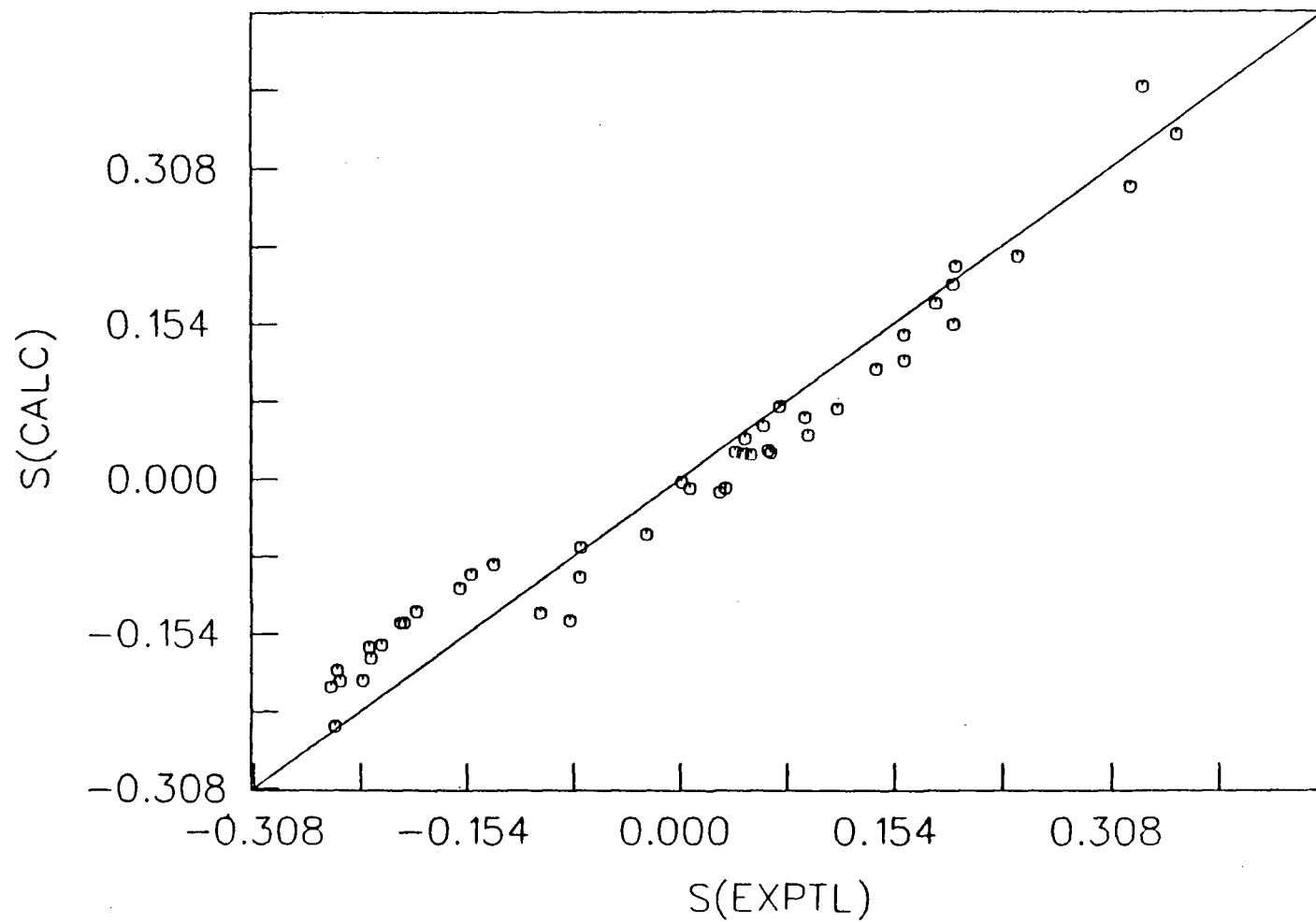tion coefficient is 0.980.

Fig. V.6   Theoretical versus scaled experimental order parameters: S_{xx}, S_{yy}, S_{zz} of solutes in 55 wt% 1132.   The value of k from this data is 5.3 dyne/cm.   Correlation coefficient is 0.979.

thesis. A comparison of Figs. V.5 and V.6 shows that the scaling did not alter the order parameter by any significant magnitude. The maximum correction in the experimental order parameters occurred for the solute 2,6-difluoropyridine and was ~5%. For the rest of the solutes, the percent change varied from 0 to 5.

The correlation coefficients indicate that the scaled results gave a slightly worse fit than the unscaled. The scaling of order parameters did not improve correlation between theory and experiment. Instead, small random scatter in the experimental parameters was introduced by the scaling. The small corrections, which may have resulted partly from errors in determining the quadrupole splittings $\Delta\nu$, cannot account for the larger deviations of theory from experiment. These results then indicate that variations among samples due to concentration and tempera- ture were either negligible or did not significantly affect the splittings in the spectrum.

V.3   Furan and Thiophene

V.3.1   Component Liquid Crystal Study

The orientation of furan and thiophene in each of the liquid crystals 1132 and EBBA was examined. In these liquid crystals, a large electric field gradient is known to be present and as such the effect of the efg-quadrupole moment mechanism is expected to be large. An attempt was made to predict the order parameters for furan and thiophene due to

the efg mechanism. The following relationship was assumed to be true, i.e. the total order parameter can be written as a sum of parameters:

$$S_{tot} = S_{efg} + S_{ss} \qquad [21]$$

where

S_{tot} is the order parameter for the solutes in the liquid crystals

S_{efg} is the order parameter due to the efg-quadrupole moment mechanism

S_{ss} is the order parameter due to the size and shape mechanism, i.e. the order parameter in 55 wt% 1132 (Table IV.3).

Calculations of the order parameters S_{tot} were done by including both mechanisms, size and shape and efg-quadrupole moment, in the size and shape program. The value of F_{ZZ} in 1132 and EBBA were obtained from a previous experiment on D_2.[19,24] The value of k was arbitrarily chosen to be the same as the unscaled k value in the 55 wt% 1132. Quadrupole moments for furan and thiophene were obtained from Ref. 59. Theoretical values of S_{efg} were then obtained by subtracting calculated S_{ss} (Table IV.3) from calculated S_{tot}. Experimental values of S_{efg} were obtained from the difference of S_{tot} (exptl) and S_{ss} (exptl).

Results for S_{efg} (calculated versus experimental) is given in Figs. V.7 and V.8 and Table V.1. The correlation between calculated and experimental values is quite good considering that there are no adjustable parameters involved, and that large errors were associated with molecular quadrupole moments used. Therefore the orientation of furan and thiophene due to the efg-quadrupole moment mechanism can be

Fig. V.7   Electric field gradient-quadrupole moment mechanism calcu-
lated versus experimental order parameters: S_{efg} of furan and
thiophene in 1132.   T = 301.4 K. F_{ZZ} (1132) = 6.067 x 10^{11}
esu. O are the order parameters of furan. + are the order
parameters of thiophene
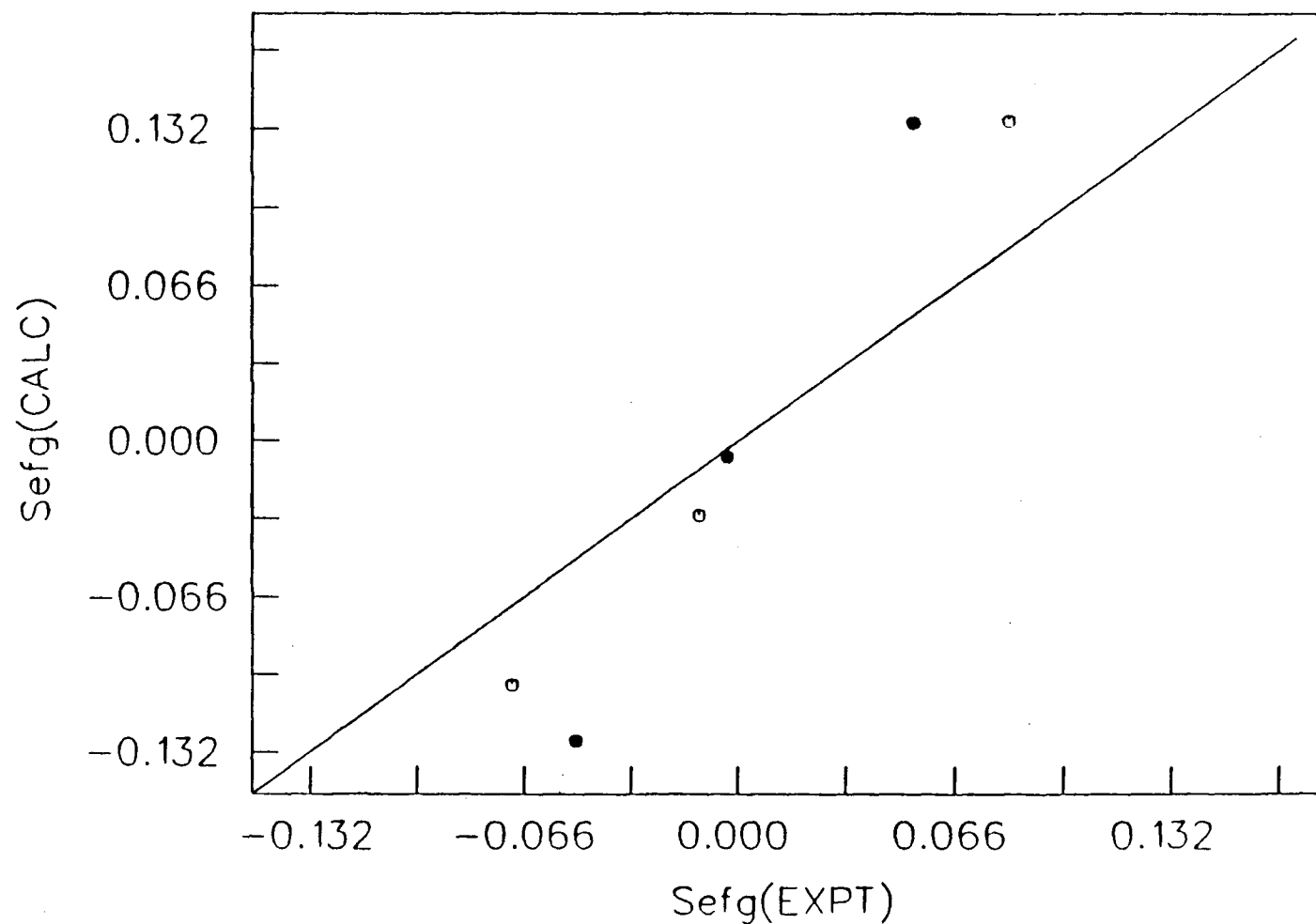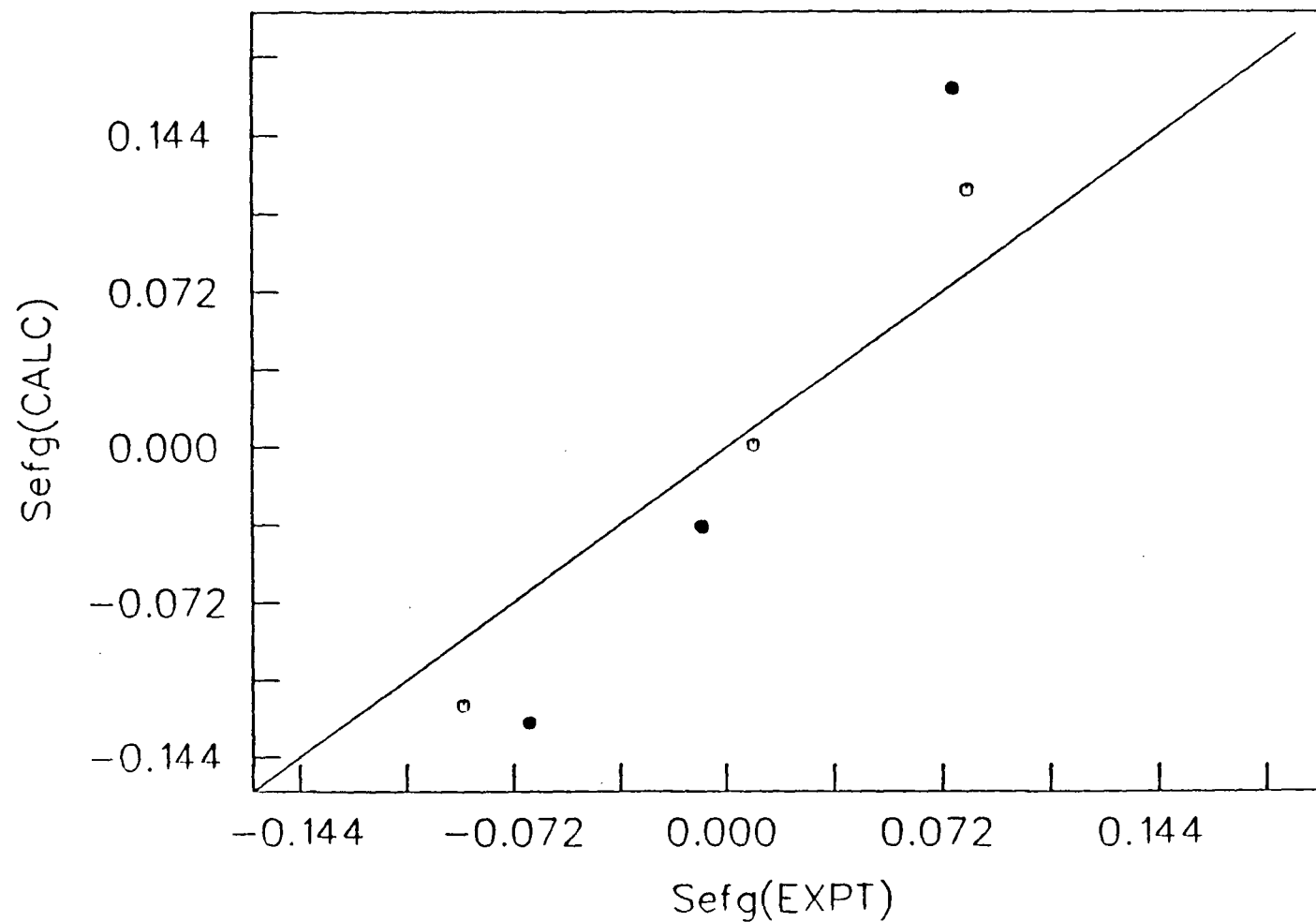
Fig. V.8   Electric field gradient-quadrupole moment mechanism calcu-
            lated versus experimental order parameters: S_{efg} of furan and
            thiophene in EBBA.   T = 301.4 K. F_{ZZ} (EBBA) = -6.420 x 10^{11}
            esu.   O are the order parameters of furan.   + are the order
            parameters of thiophene

Table V.1:   Electric field gradient-quadrupole moment mechanism:
              calculated[a] and experimental order parameters of furan and
              thiophene in 1132 and EBBA.

| Liquid Crystal | | Order Parameters[b] (S_{efg}) | | | |
| | | Furan | | Thiophene | |
		Experimental	Calculated	Experimental	Calculated
1132	S_{xx}	0.0820 (2)	0.1352	0.0532 (2)	0.1342
	S_{yy}	-0.0122 (5)	-0.0318	-0.0034 (10)	-0.0069
	S_{zz}	-0.0698 (3)	-0.1034	-0.0500 (8)	-0.1273
EBBA	S_{xx}	-0.0890 (2)	-0.1198	-0.0668 (4)	-0.1280
	S_{yy}	0.0090 (6)	0.0012	-0.0086 (18)	-0.0367
	S_{zz}	0.0800 (4)	0.1186	0.0753 (14)	0.1647

[a]   Quadrupole moment of furan and thiophene were obtained from Ref. 59.

      k = 5.2 dyne/cm, assumed to be the same as in 55 wt% 1132.

      F_{ZZ} (1132) = 6.067 x 10^{11} esu

      F_{ZZ} (EBBA) = -5.748 x 10^{11} esu

[b]   Equation [21]: $S_{efg} = S_{tot} - S_{ss}$

      S_{tot} = order parameter in component liquid crystals

      S_{efg} = order parameter due to efg-quadrupole moment mechanism.

      S_{ss} = order parameter due to size and shape mechanism (value

              from 55 wt% 1132.

predicted fairly well. The orientation of these two molecules in these liquid crystals can be explained using the two mechanisms: size and shape, and efg-quadrupole moment. This piece of evidence ties in with van der Est's results[22] which show that the orientation of molecules can be explained using these mechanisms.

V.3.2   Temperature Study

The orientation of furan and thiophene in 55 wt% 1132 was studied as a function of temperature. The temperature range chosen: 304-325 K (dial T), is within the nematic phase of the liquid crystalline mixture. The magnitude of the order parameters for both solutes were found to decrease steadily with increase of temperature (Table IV.6, Figs. V.9 to V.14). This is expected because at higher temperatures, the liquid crystal molecules possess more thermal energy, thus exhibiting more motion. As a result, the ordering of these molecules is lowered which in turn reduces the orientational order in the solutes.

The temperature dependence of S was calculated using the size and shape program. The efg-quadrupole moment mechanism was included in addition to the size and shape interaction. The efg at each temperature were determined from D_2 experiments. Furan and thiophene were assumed to experience the same efg as D_2 at these temperatures. Quadrupole moments were obtained from Ref. 59. The values of k for different temperatures were estimated by scaling with the quadrupolar splittings

of EBBA. Here k is assumed to vary proportionally with the orientation of the C-D bond direction of EBBA.

$$k_T = \frac{\Delta\nu_T}{\Delta\nu_{301.4}} \times k_{301.4} \qquad [22]$$

where

k_T is the force constant at temperature T.

$k_{301.4}$ is the force constant obtained from unscaled results at temperature 301.4 K.

$\Delta\nu_T$ is the quadrupolar splitting of EBBA at temperature T.

$\Delta\nu_{301.4}$ is the splitting at 301.4 K.

The calculated results are plotted in Figs. V.9 to V.14.

At a first glance, the magnitude of the predicted order parameters appears to be quite different from that of experimental results. This difference is, however, of the same magnitude as that in the whole series of solutes. The probable factors causing these deviations have been discussed in Section V.2.2. On the other hand, the temperature dependence of the order parameters is generally well-predicted. Calculated and experimental values of S_{xx} and S_{yy} decrease with temperature. Both theoretical and observed S_{zz} values increase with increase of temperature.

The correlation between theory and experiment of the temperature dependence of S is quite good indicating that the assumptions made regarding the temperature dependence of efg and k were reasonable. Furan and thiophene were assumed to experience the same variation in efg

with temperature as D_2 molecules. In the context of the model, the exact dependence of k on $\Delta\nu_T$ and temperature is not known. As temperature increases, ordering of liquid crystal molecules decreases, thus less force is needed to push the walls of the elastic tube apart. The force constant should then decrease. It seemed reasonable to assume that k should vary proportionally with $\Delta\nu_T$ as temperature is changed. The results show this to be valid. The change in orientational behavior of furan and thiophene in the 55 wt% 1132 can be explained by the two mechanisms: efg-quadrupole moment, and size and shape.
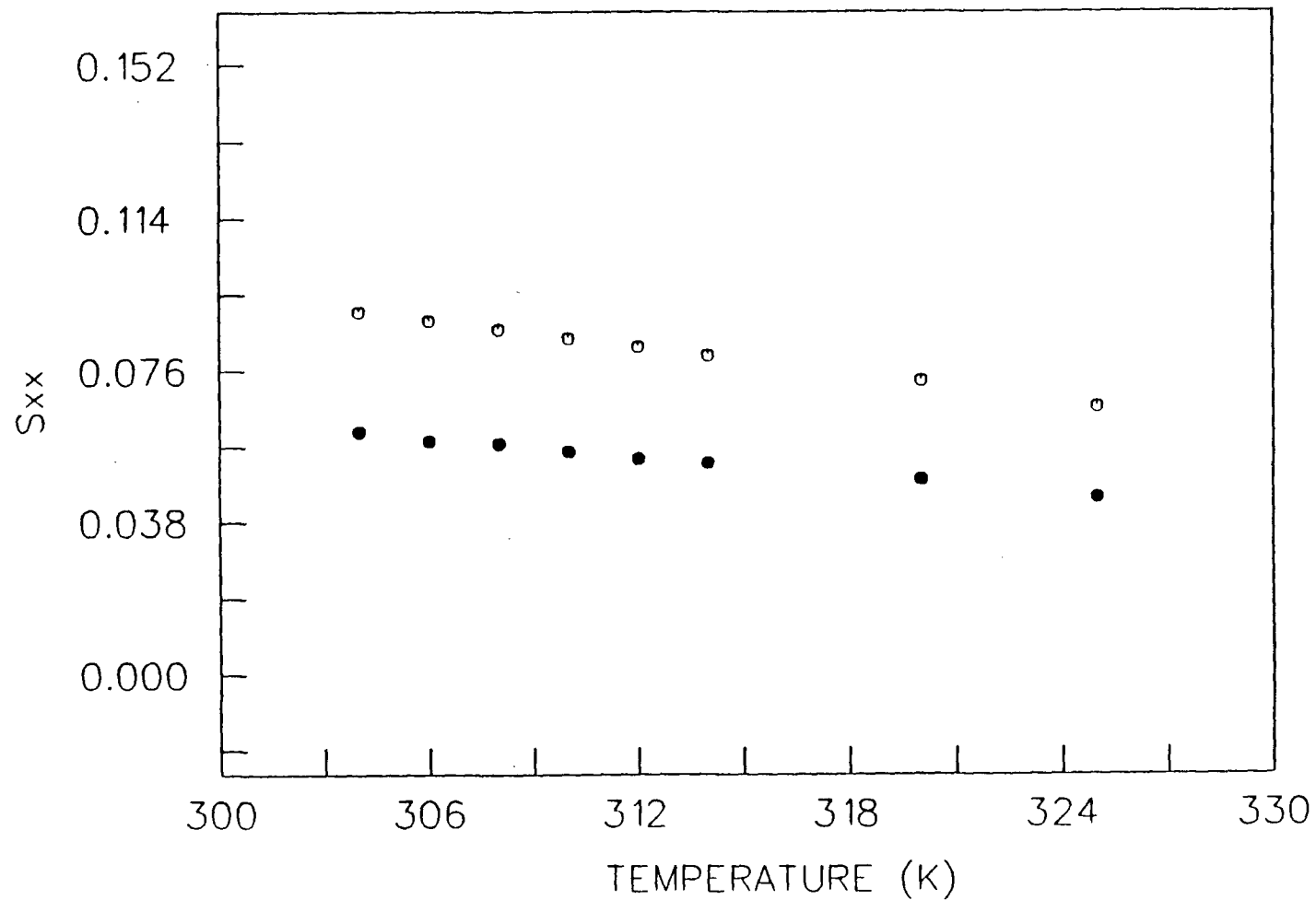
Fig. V.9   Temperature dependence of the order parameters S_{xx}
(calculated and experimental) of furan in 55 wt% 1132
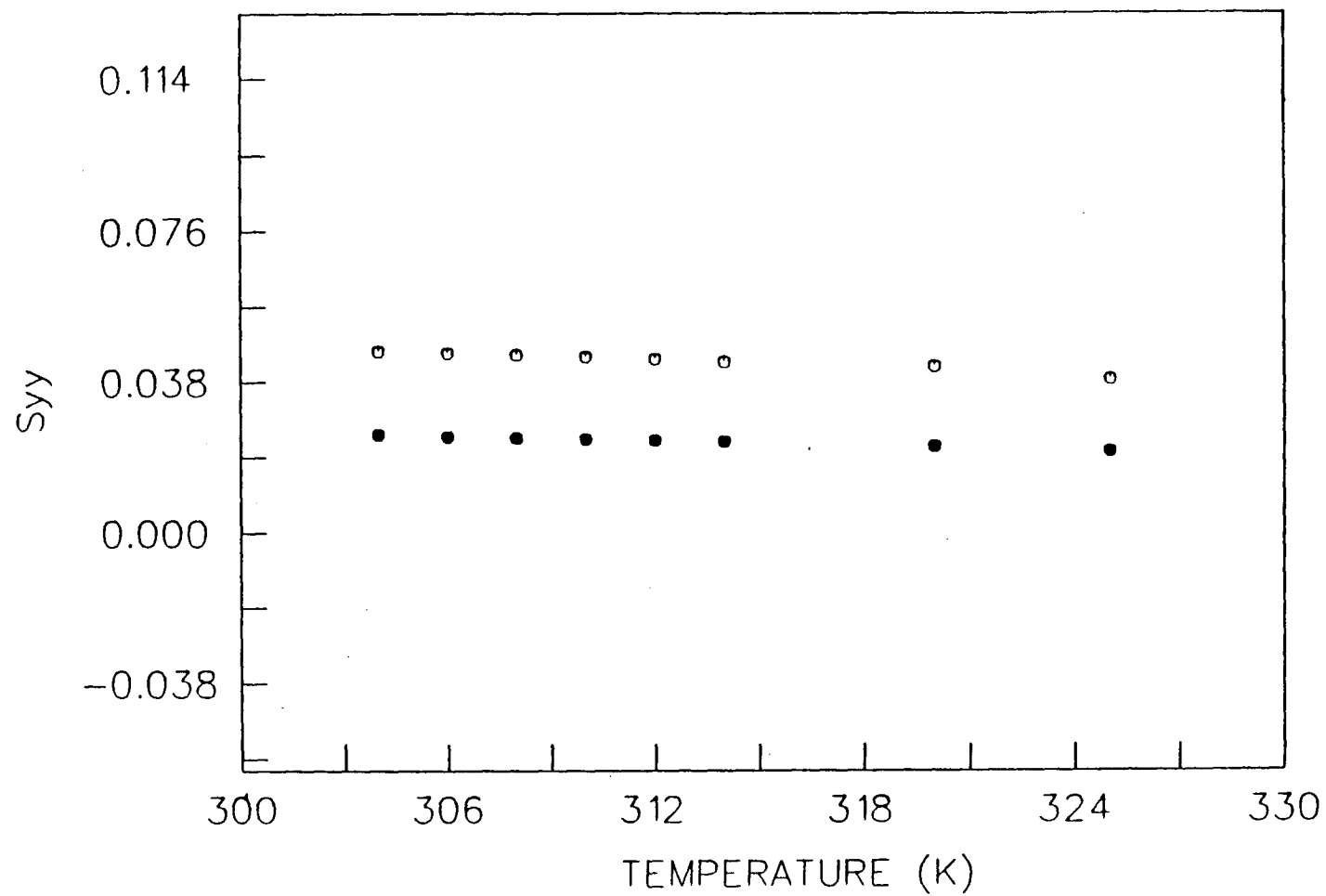⊙ refers to the experimental results
● refers to the calculated results

Fig. V.10 Temperature dependence of the order parameters S_{yy} calculated and experimental) of furan in 55 wt% 1132
○ refers to the experimental results
● refers to the calculated results

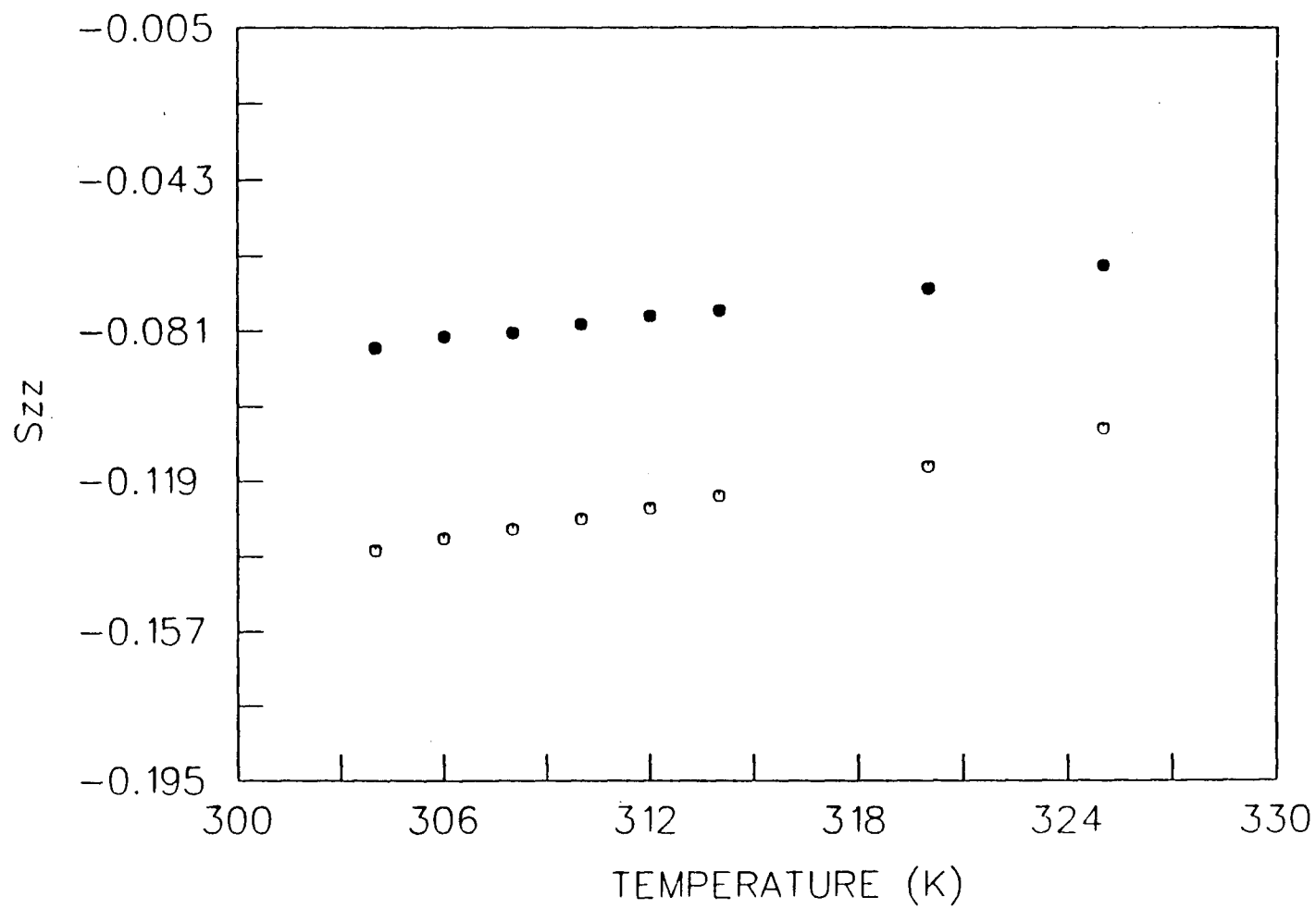Fig. V.11   Temperature dependence of the order parameters: S_{zz} -
calculated (●) and experimental (◉), of furan in 55 wt% 1132

Fig. V.12   Temperature dependence of the order parameters: S_{xx}-
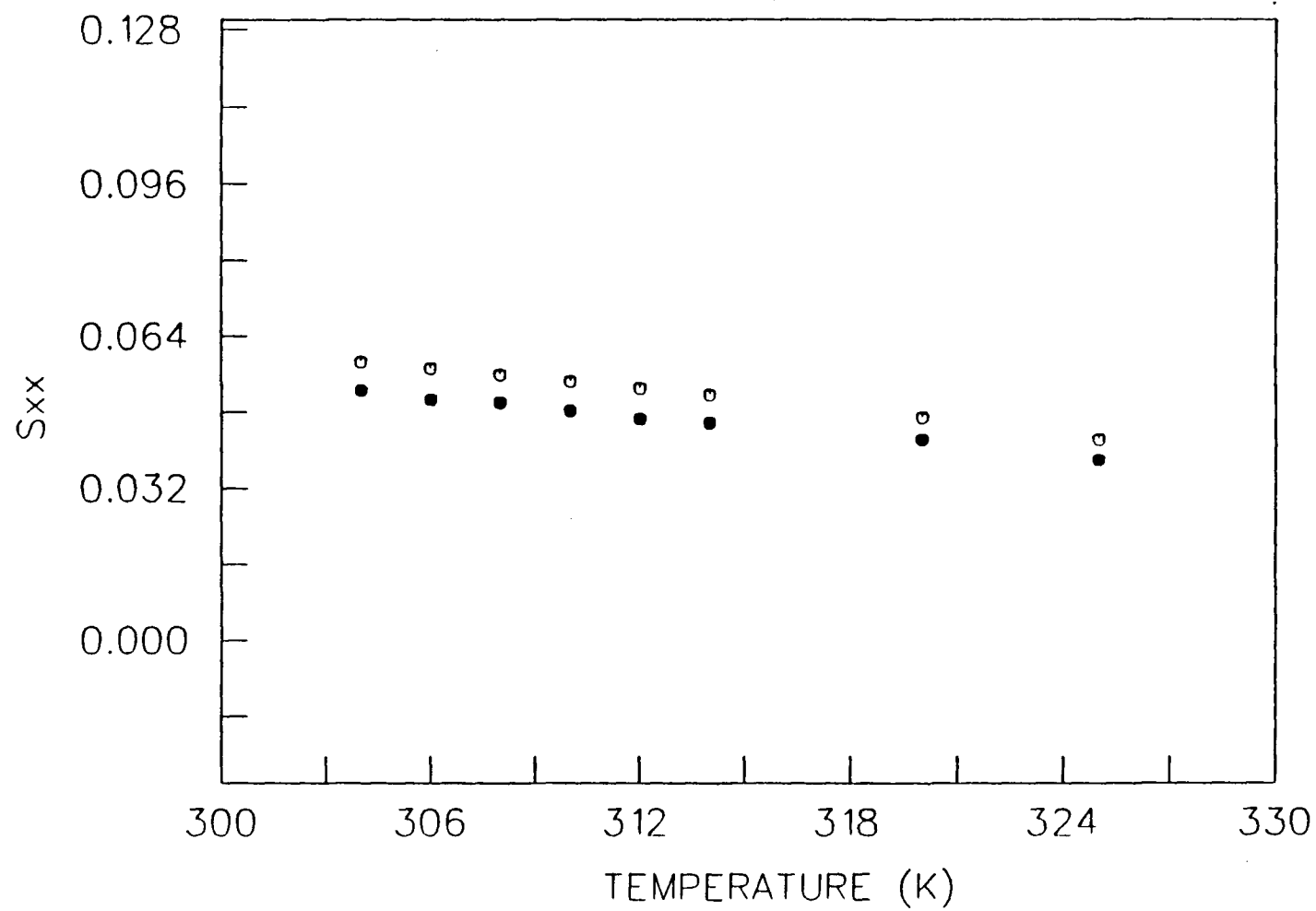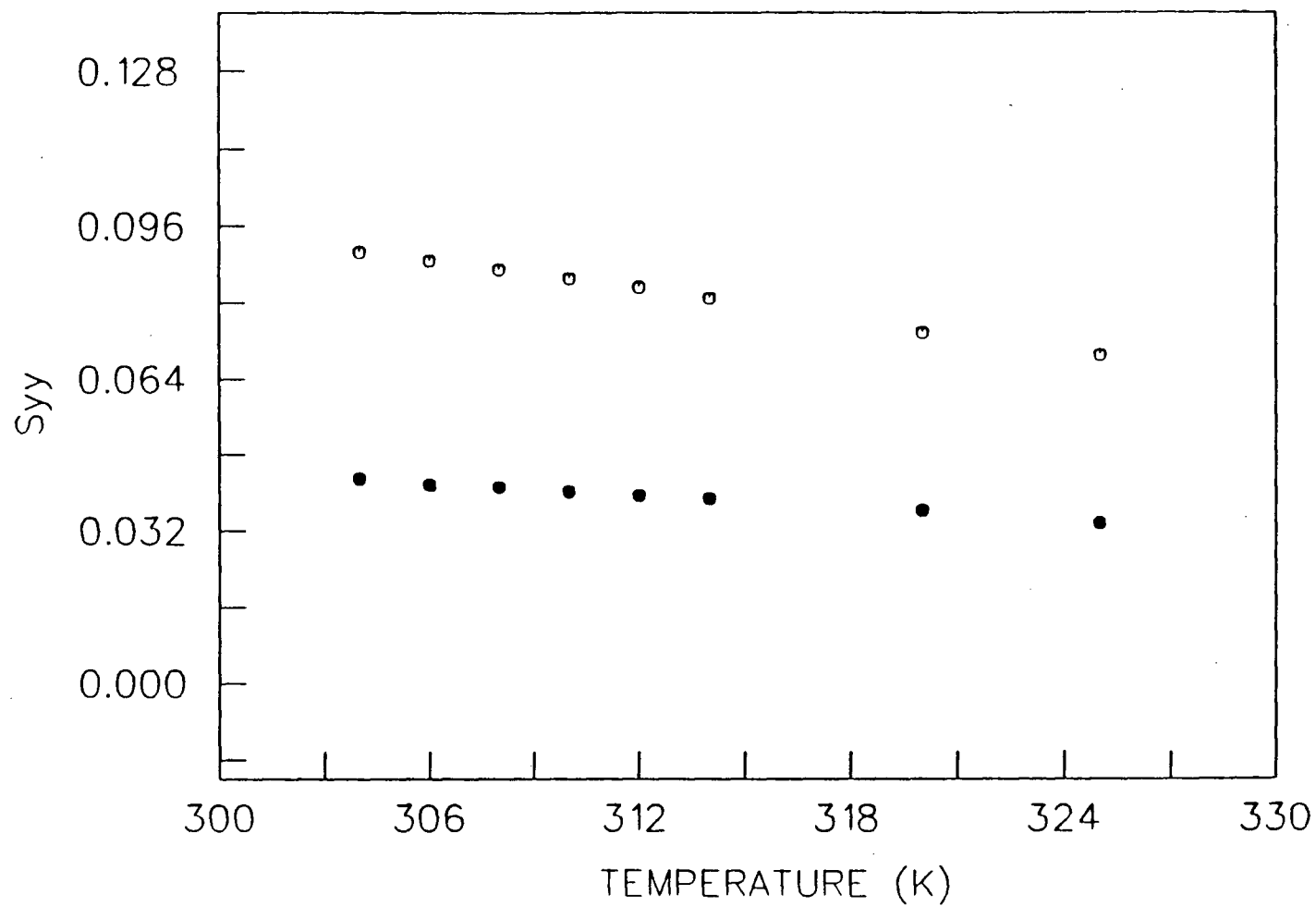calculated (●) and experimental (◎), of thiophene in 55 wt%
1132

Fig. V.13 Temperature dependence of the order parameters: S_{yy}-calculated (●) and experimental (⊙), of thiophene in 55 wt% 1132
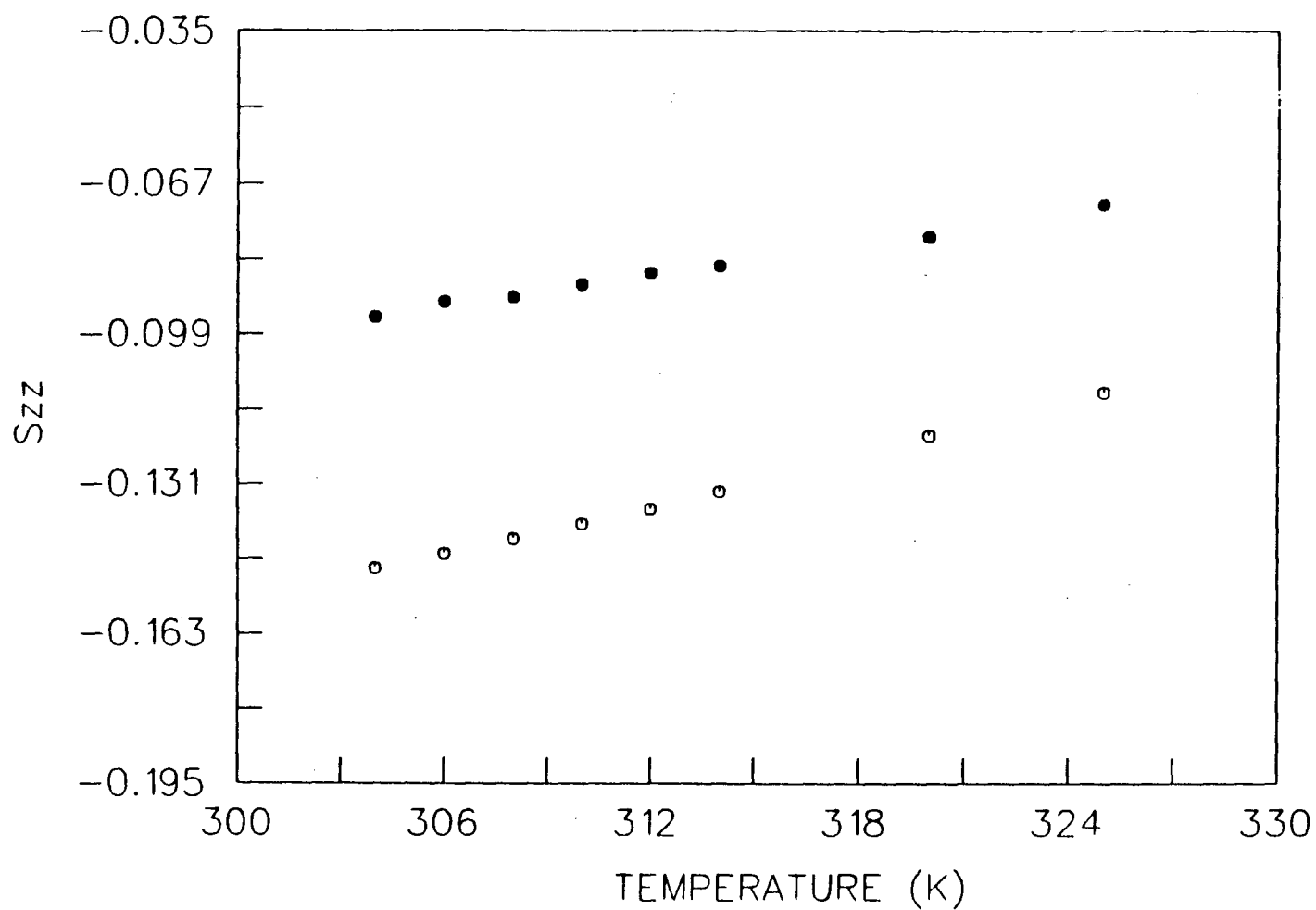
Fig. V.14   Temperature dependence of the order parameters: S_{zz}-
calculated (●) and experimental (○), of thiophene in 55 wt%
1132

CHAPTER VI

CONCLUSION

VI.   CONCLUSION

The results of a series of C_{2v}^* molecules in 55 wt% 1132 indicate that in this liquid crystal, orientation parameters of solutes depend on their dimensions. The model based on short range hard body interactions (dependent on the size and shape of solutes) is successful in describing the orientational behavior of solutes. Order parameters calculated are in good agreement with experiment despite the various assumptions associated with the model. These results support the conclusion that orientation of solutes in 55 wt% 1132 is dominated by short range hard body interactions. The temperature dependence of ordering in 55 wt% 1132, and orientation in 1132 and EBBA, were well predicted with the inclusion of the electric field gradient-quadrupolar moment mechanism in addition to short range hard body interactions.

CHAPTER VII

BIBLIOGRAPHY

VII.   BIBLIOGRAPHY

1. J.W. Emsley,   Nuclear Magnetic Resonance of liquid Crystals,   D. Reidel Publishing Company (1985).

2. G.R. Luckhurst and G.W. Gray,   Molecular Physics of Liquid Crystals, Academic Press (1979).

3. E.E. Burnell and C.A. de Lange,   Phys. Rev. A25, 2339 (1982).

4. F. Reinitzer,   Monatsh, 9, 421 (1888).

5. O. Lehmann. "Flussige Kristalle, sowie Plastizitat von Kristallen im Allgemeinen, molekulare Umlagerungen und Aggregatzustand sanderungen" Engelmann, Liepzig, (1904).

6. G.R. Luckhurst,   Quart. Rev. 22, 179 (1968).

7. A. Saupe and G. Englert,   Phys. Rev. Lett. 11, 462 (1963).

8. G. Englert and A. Saupe,   Z. Naturforsch. 19a, 172 (1964).

9. P. Diehl, C.L. Khetrapal,   NMR Basic Principles and Progress 1, 1 (1969).

10. A. Saupe,   Mol. Cryst. 1, 231 (1971).

11. J.C. Robertson, C.T. Yim,   and D.F.R. Gilson,   Can. J. Chem. 49, 2345 (1971).

12. E.T. Samulski,   Ferroelectrics 31, 83 (1980).

13. J.M. Anderson,   J. Magn. Reson. 4, 231 (1971).

14. J.G. Snijders, C.A. de Lange, and E.E. Burnell,   Israel J. Chem. 23, 269 (1983).

15. E.E. Burnell and C.A. de Lange,   J. Chem. Phys. 76, 3474 (1982).

16. J.G. Snijders, C.A. Lange, and E.E. Burnell,   J. Chem. Phys. 77, 5386 (1982).

17. J.G. Snijders, C.A. Lange, and E.E. Burnell,   J. Chem. Phys. 79, 2964 (1983).

18. A.J. van der Est, P.B. Barker, E.E. Burnell, C.A. de Lange, and J.G. Snijders,   Mol. Phys. 56, 161 (1985).

19. G.N. Patey, E.E. Burnell, J.G. Snijders, and C.A. de Lange,   Chem. Phys. Lett. 99, 271 (1983).

20. P.B. Barker, A.J. van der Est, E.E. Burnell, C.A. de Lange, and J.G. Snijders, Chem. Phys. Lett. **107**, 426 (1984).

21. R.F. Code and W.F. Ramsey, Phys. Rev. **A4**, 1945 (1971).

22. A.J. van der Est, M.Y. Kok, and E.E. Burnell, Mol. Phys. (in press).

23. J.W. Emsley, J.C. Lindon, NMR Spectroscopy Using Liquid Crystals, Pergamon Press, (1975).

24. A.J. van der Est, private communication.

25. J. Lounila and J. Jokisaari, Progr. in NMR Spectrosc. **15**, 249 (1982).

26. N.H. Werstiuk, T. Kadai, Can. J. Chem. **52**, 2169 (1974).

27. P. Keller and L. Liebert, Solid State Physics, **14**, 20 (1978).

28. Kodak Publication No. JJ-14, EASTMAN Liquid Crystal Products, (1973).

29. P. Diehl, H. Kellerhals, E. Lustig, NMR Basic Principles and Progress **6**, 1 (1972).

30. P. Diehl, P.M. Henrichs, and W. Niederberger, Mol. Phys. **20**, 139 (1971).

31. T.C. Wong, E.E. Burnell, and L. Weiler, Chem. Phys. Lett. **50(2)**, 243 (1977).

32. M.S. Gopinathan and P.T. Narasimhan, J. Magn. Reson. **6**, 147 (1972).

33. R.C. Long, Jr., S.L. Baugheum, and J.H. Goldstein, J. Magn. Reson. **7**, 253 (1972).

34. J.M. Read, Jr., C.T. Mathis, and J.H. Goldstein, Spectrochim. Acta **21**, 85 (1965).

35. E.E. Burnell and C.E. de Lange, Mol. Phys. **16(1)**, 95 (1969).

36. W.A. Thomas and G.E. Griffin, Org. Magn. Reson. **2**, 503 (1970).

37. J. Gerritsen and C. Maclean, Recueil, **91**, 1393 (1972).

38. H.B. Evans, Jr., A.R. Tarpley, and J.H. Goldstein, J. Phys. Chem. **72(7)**, 2552 (1968).

39. P. Diehl and C.L. Khetrapal, Mol. Phys. **15**, 201 (1968).

40. P. Diehl, J. Amrein, H. Bosinger, and F. Moia, Org. Magn. Reson. 18(1), 21 (1982).

41. J.M. Read, Jr., R.W. Crecely, R.S. Butler, J.E. Loemker, and J.H. Goldstein, Tet. Lett. 10, 1215 (1968).

42. W.A. Tallon and G.B. Savitsky, J. Magn. Reson. 9, 422 (1973).

43. E.E. Burnell and M.A. Sweeney, Can. J. Chem. 52(21), 2565 (1974).

44. E.E. Burnell, P. Diehl, and W. Neiderberger, Can. J. Chem. 52, 151 (1974).

45. L.E. Sutton, Table of Interatomic Distances, Special Publication No. 11, Chem. Soc. London, (1958).

46. B. Bak, D. Christensen, W.B. Dixon, L. Hansen-Nygaard, J.R. Andersen, and M. Schotlander, J. Mol. Spectrosc. 9, 124 (1962).

47. B. Bak, D. Christensen, L. Hansen-Nygaard, and J.R. Andersen, J. Molec. Spectrosc. 7, 58 (1961).

48. B. Bak, L. Hansen-Nygaard, and J.R. Andersen, J. Molec. Spectrosc. 2, 361 (1958).

49. O.L. Stiefvater, Z. Naturforsch. 30a, 1765 (1975).

50. L. Nygaard, J. Bojesen, T. Pedersen, and J.R. Andersen, J. Mol. Struct. 2, 209 (1968).

51. F. Michel, H. Nery, G. Roussy, Compt. Rendu 278B, 203 (1974).

52. Harmony et al., J. Phys. Chem. Ref. Data. 8, 717 (1979).

53. M. Onda and I. Yamaguchi, J. Molec. Struct. 34, 1 (1976).

54. M. Onda, O. Ohashi, and I. Yamaguchi, J. Molec. Struct. 31, 203 (1976).

55. O.G. Batyukhnova, N.I. Sadova, L.V. Vilkov, Yu. A. Pankrushev, J. Molec. Struct. 97, 153 (1983).

56. J. Trotter and C.S. Williston, Acta Cryst. 21, 285 (1966).

57. A. Bondi, J. Phys. Chem. 68, 441 (1964).

58. A.D. Buckingham, E.E. Burnell, and C.A. de Lange, J. Amer. Soc. 90, 2972 (1968).

59. G. de Broukere, W.C. Nieuwpoort, R. Broer, and G. Berthier, Mol. Phys. 45, 649 (1982).

APPENDIX

APPENDIX

Experimental order parameters of solutes dissolved in 55 wt% 1132 at 301.4 K (the EBBA molecules in the mixture were not deuterated)

	Molecule		Experimental Order Parameter
1	TTF	S_{xx}	0.3320 (17)
		S_{yy}	-0.081 (3)
		S_{zz}	-0.2514 (17)
2	Furan	S_{xx}	0.0914 (1)
		S_{yy}	0.0460 (3)
		S_{zz}	-0.1374 (2)
3	Thiophene	S_{xx}	0.0604 (1)
		S_{yy}	0.0922 (4)
		S_{zz}	-0.1526 (3)
4	Pyridine	S_{xx}	0.1178 (2)
		S_{yy}	0.0444 (5)
		S_{zz}	-0.1622 (3)
5	2,6-Difluoropyridine	S_{xx}	0.1640 (3)
		S_{yy}	0.0379 (6)
		S_{zz}	-0.2019 (3)

6	Fluorobenzene	S_{xx}	0.0513 (1)
		S_{yy}	0.1411 (2)
		S_{zz}	-0.1924 (1)
7	Iodobenzene	S_{xx}	-0.0238 (3)
		S_{yy}	0.2355 (7)
		S_{zz}	-0.2117 (4)
8	1,2-Dicyanobenzene	S_{xx}	0.0610 (10)
		S_{yy}	0.1770 (22)
		S_{zz}	-0.2380 (12)
9	1,3-Dinitrobenzene	S_{xx}	-0.1915 (21)
		S_{yy}	0.0320 (4)
		S_{zz}	-0.2236 (14)
10	1,4-Dichlorobenzene	S_{xx}	-0.0711 (1)
		S_{yy}	0.3148 (4)
		S_{zz}	-0.2437 (3)
11	1,4-Dibromobenzene	S_{xx}	-0.0988 (1)
		S_{yy}	0.3465 (2)
		S_{zz}	-0.2477 (1)